UCRL-17314

University of California

Ernest O. Lawrence Radiation Laboratory

CALCULATION OF STOPPING POWER AND RANGE-ENERGY VALUES FOR ANY HEAVY ION IN NONGASEOUS MEDIA

TWO-WEEK LOAN COPY

This is a Library Circulating Copy which may be borrowed for two weeks. For a personal retention copy, call Tech. Info. Division, Ext. 5545

Berkeley, California

DISCLAIMER

This document was prepared as an account of work sponsored by the United States Government. While this document is believed to contain correct information, neither the United States Government nor any agency thereof, nor the Regents of the University of California, nor any of their employees, makes any warranty, express or implied, or assumes any legal responsibility for the accuracy, completeness, or usefulness of any information, apparatus, product, or process disclosed, or represents that its use would not infringe privately owned rights. Reference herein to any specific commercial product, process, or service by its trade name, trademark, manufacturer, or otherwise, does not necessarily constitute or imply its endorsement, recommendation, or favoring by the United States Government or any agency thereof, or the Regents of the University of California. The views and opinions of authors expressed herein do not necessarily state or reflect those of the United States Government or any agency thereof or the Regents of the University of California.

Research and Development

UCRL-17314
UC-34 Physics
TID-4500 (49th Ed.)

UNIVERSITY OF CALIFORNIA

Lawrence Radiation Laboratory
Berkeley, California

AEC Contract No. W-7405-eng-48

CALCULATION OF STOPPING POWER AND RANGE-ENERGY VALUES FOR ANY HEAVY ION IN NONGASEOUS MEDIA

Palmer G. Steward and Roger Wallace

December 20, 1966

CALCULATION OF STOPPING POWER AND RANGE-ENERGY VALUES FOR ANY HEAVY ION IN NONGASEOUS MEDIA

Contents

Abstract v
I. Introduction 1
II. Method
A. Method For Z Less Than Ten 2
B. Method For Z Greater Than Ten 7
III. Discussion of Method
A. Z Less Than Ten 12
B. Z Greater Than Ten 14
IV. Results 19
V. Acknowledgment 23
VI. Bibliography 24

CALCULATION OF STOPPING POWER AND RANGE-ENERGY VALUES FOR ANY HEAVY ION IN NONGASEOUS MEDIA

Palmer G. Steward and Roger Wallace

Lawrence Radiation Laboratory
University of California
Berkeley, California

December 20, 1966

ABSTRACT

A method is presented for calculating range-energy and stopping-power data for any heavy ion with $0.01 \leq \epsilon \leq 500$ MeV/amu incident upon any nongaseous stopping medium. The method is incorporated into a FORTRAN computer program. Results for H, ^{4}He, ^{12}C, ^{20}Ne, ^{40}Ar, ^{84}Kr, ^{131}Xe, and ^{238}U ions each incident upon H_2O, Al, Cu, Ag, Pb, and U are presented.

For ions with $Z \leq 10$, the program uses experimental data and a modified version of Northcliffe's method at low energy. For ions with $Z > 10$, the nuclear and electronic stopping-power theory developed by Lindhard et al. is adjusted to fission-product range data at low energy; for intermediate-energies, charge-state data developed from experimental Ar range-energy data in Al is extended to other ions and stopping media. A somewhat modified Bethe's theory used by Barkas and Berger is used here for all ions at high energy. The particle ranges presented here are merely the integral of the inverse of the stopping power and do not include the effects of high-energy multiple scattering.

I. INTRODUCTION

The proposed Omnitron will make available for experimental study heavy ions that are presently unavailable. The behavior, in a stopping material, of ions with energies greater than 10 MeV/amu and with Z number greater than 18 has not been thoroughly investigated either theoretically or experimentally in the past, because no means of attaining these ions has been available. Now, the possibility that this accelerator may make available such ions for use in radiobiology has stimulated a need to generate range-energy and stopping-power data in any arbitrary medium for ion energies up to 500 MeV/amu and Z numbers through 92.

In this paper, we propose a method of synthesizing this data from presently available experimental and theoretical studies, and present the results of stopping-power calculations using the method. We believe that any such results contain some degree of uncertainty and thus some adjustments in the data presented is inevitable as experimental data from the accelerator becomes available.

The method, which is proposed below, for obtaining this range-energy and stopping-power data is designed to be conveniently incorporated into a computer program. This program may be used as a subroutine of a main program in which this data is required, or it may be used alone to produce range-energy and stopping-power tables. The method is also designed to give results of adequate accuracy for the general case, i.e., for arbitrary ion atomic number and atomic weight and arbitrary nongaseous stopping medium. More accurate results for particular ions and stopping media can occasionally be found elsewhere, when either experimental data is available or a specialized theory good for the particular case in question has been used.

Experimental stopping-power data are available for ions with $Z < 10$ for all energies for which the atom is not completely stripped of electrons. Data for such energies with $Z > 10$, which are difficult to treat theoretically, are incomplete. Therefore, it is convenient to consider the problem separately for $Z \leq 10$ and for four separate energy regions with $Z > 10$.

We first consider the low-energy region in which there is some fission-product data and in which stopping-power theory developed for fission products is valid. This region is defined by $137\ \beta \leq Z^{1/3}$, where β is the ratio of the ion velocity to the speed of light. The second is the high-energy region in which the atoms are completely stripped of orbital electrons. This region is defined by $137\ \beta > 3Z$. The third is the medium-high-energy region in which some charge-state data can be generated. Here $9 < 137\ \beta \leq 3Z$, where $137\ \beta = 9$ corresponds to an energy of 2 MeV/amu. In the fourth energy region for which $Z^{1/3} < 137\ \beta \leq 9$, there is no experimental data and no acceptable theory available. This we call the medium-low-energy region. It is a narrow region in which a cubic polynomial, which matches the slope and magnitude of the stopping power at both boundaries is quite adequate for our purposes.

II. METHOD

A. Method for Z Less Than Ten

Since experimental and theoretical stopping-power data exist for ions with $Z \leq 10$, it is convenient to calculate stopping power separately for these ions by using a method that can optimize the use of these data. Charge exchange is a significant process only for particles of less than 10 MeV/amu with $Z \leq 10$. Thus we calculate stopping power for these lower-energy ions separately, using a method proposed by Northcliffe[1] with some minor modifications. For energies greater than 10 MeV/amu the proton stopping-power data of Barkas and Berger[2] are extended to heavier ions by using the relative stopping-power formula for two ions of the same velocity,

$$-\frac{dE}{dX} = Z^2 \left(-\frac{dE}{dX}\right)_p , \qquad (1)$$

where Z is the atomic number of the ion, and $-(dE/dX)_p$ is the proton stopping power in units of MeV/g-cm^{-2}.

1. Energy Less Than 10 MeV/amu

Let us designate the ion and stopping medium for which we want the stopping power by their atomic numbers Z and Z_t, respectively. Let us designate the stopping power for ion Z in medium Z_t by

dE^Z/dX_{Z_t}, the superscript representing the ion, and the subscript the stopping medium.

First we calculate the relative stopping power for protons in two different stopping media. One medium is Z_t, the other is Al. That is, we calculate as a function of energy the relative stopping power for protons

$$\frac{dE^1}{dX_{Z_t}} \Big/ \frac{dE^1}{dX_{13}} .$$

This quantity is calculated in four steps. First, we find the relative stopping power at 2 and at 10 MeV/amu. Second, from these two points the constants p and q are found where

$$\frac{dE^1}{dX_{Z_t}} \Big/ \frac{dE^1}{dX_{13}} = p\epsilon^q ,$$

where ϵ is the energy in units of MeV/amu. We assume that this function is the same for $1 \leq Z \leq 10$, so that

$$\frac{dE^Z}{dX_{Z_t}} \Big/ \frac{dE^Z}{dX_{13}} = p\epsilon^q . \qquad (2)$$

Third, using a formula for electronic stopping power derived by Lindhard and Scharff[3] using the Thomas-Fermi atomic model, we predict that in the limit of low energy this relative stopping power is the constant

$$K = \frac{27}{13} \frac{Z_t}{A_t} \frac{(Z^{2/3} + 13^{2/3})^{3/2}}{(Z^{2/3} + Z_t^{2/3})^{3/2}} . \qquad (3)$$ *

---

*When there are several atomic components in the stopping medium, this expression becomes

$$K = \frac{27}{13} (Z^{2/3} + 13^{2/3})^{3/2} \rho \sum_{i=1}^{N} \frac{Z_{t_i}}{A_{t_i}} \frac{\rho_i}{(Z^{2/3} + Z_{t_i}^{2/3})^{3/2}} .$$

Here there are N atomic components,

$$\rho_i = \rho \frac{n_i A_{t_i}}{\sum_{i=1}^{N} n_i A_{t_i}} ,$$

where n_i is the relative abundance of the ith component, ρ is the density of the stopping medium, and Z_{t_i} and A_{t_i} are respectively the atomic number and atomic weight of the ith component. The effect of chemical binding is ignored.

Fourth, we solve for the intersection of Eqs. (2) and (3), that is we solve for ϵ_0, where $p\epsilon_0^q = K$. Then the relative stopping power is

$$\frac{dE^Z}{dX_{Z_t}} \Big/ \frac{dE^Z}{dX_{13}} = p\epsilon^q \qquad (\epsilon > \epsilon_0) \tag{4a}$$

and

$$\frac{dE^Z}{dX_{Z_t}} \Big/ \frac{dE^Z}{dX_{13}} = K \qquad (\epsilon \leq \epsilon_0). \tag{4b}$$

To calculate the relative stopping power for protons at 2 and 10 MeV/amu required in step one above, we use

$$-\frac{dE^1}{dX_{13}} = 112.31 \text{ MeV/g-cm}^{-2}$$

at $\epsilon = 2.0$ MeV/amu and

$$-\frac{dE^1}{dX_{13}} = 34.28 \text{ MeV/g-cm}^{-2}$$

at $\epsilon = 10.0$ MeV/amu together with Barkas and Berger's polynomial approximations to Bethe's theory.[2] The polynomials (for protons only) are

$$-\frac{dE}{dX} = \frac{\epsilon}{\lambda}\left\{\sum_{n=1}^{2}\sum_{m=0}^{2} n\,\alpha_{mn}(\log I_{adj})^m(\log\epsilon)^{n-1}\right\}^{-1} \qquad (1 \leq \epsilon \leq 7 \text{ MeV}), \tag{5A}$$

where

$$\log\lambda = \log\frac{A_t}{Z_t} + \sum_{n=0}^{2}\sum_{m=0}^{2}\alpha_{mn}(\log I_{adj})^m(\log\epsilon)^n - 3\log 10; \tag{5B}$$

and

$$-\frac{dE}{dX} = \frac{\epsilon}{\lambda}\left\{\sum_{n=1}^{3}\sum_{m=0}^{3} n\,\alpha_{mn}(\log I_{adj})^m(\log\epsilon)^{n-1}\right\}^{-1} \qquad (7 \leq \epsilon \leq 1200 \text{ MeV}) \tag{6A}$$

where

$$\log \lambda = \log \frac{A_t}{Z_t} + \sum_{n=0}^{3} \sum_{m=0}^{3} \alpha_{mn} (\log I_{adj})^m (\log \epsilon)^n.^{*} \qquad (6B)$$

In Eqs. (5) and (6), I_{adj} is the mean ionization energy of the stopping medium in units of eV, adjusted for use in Barkas and Berger's work as discussed in reference 2, λ is the proton range in units of g/cm^2, and $-(dE/dX)$ is in units of $MeV/g\text{-}cm^{-2}$. The coefficients a_{mn} and α_{mn} as determined by Barkas and Berger are given in Tables I and II, respectively.

Finally, to calculate the stopping power for $\epsilon \leq 10$ MeV/amu and $Z \leq 10$ in any Z_t, we multiply the relative stopping power of Eq. (4) by the accurate, experimentally determined stopping power of ions in Al. Northcliffe[1] has placed smooth curves through this stopping-power data in aluminum, which is presented in Fig. 1.

2. Energies Greater than 10 MeV/amu

The ions are completely stripped of orbital electrons for $Z \leq 10$ and $\epsilon > 10$ MeV/amu, so we can use Eqs. (1) and (6) to calculate the stopping power directly. Thus we have

$$-\frac{dE^Z}{dX_{Z_t}} = Z^2 \left(-\frac{dE^1}{dX_{Z_t}} \right), \qquad (7)$$

where $-dE^Z/dX_{Z_t}$ is the desired stopping power in units of $MeV/g\text{-}cm^{-2}$ of ion Z in the stopping medium Z_t, and $-dE^1/dX_{Z_t}$ is the proton stopping power in Z_t as given by Eq. (6).

The range of the charged particle in g/cm^2 is easily calculated from

---

*When there are several atomic components in the stopping medium, the expression for $\frac{A_t}{Z_t}$ becomes

$$\frac{A_t}{Z_t} = \left[\frac{1}{\rho} \sum_{i=1}^{N} \rho_i \frac{Z_{t_i}}{A_{t_i}} \right]^{-1},$$

where the symbols are defined in the previous footnote.

Table I. Coefficients a_{mn} for Eq. (5).

m/n	n = 0	n = 1	n = 2
0	-7.5265×10^{-1}	2.5398	-2.4598×10^{-1}
1	7.3736×10^{-2}	-3.12×10^{-1}	1.1548×10^{-1}
2	4.0556×10^{-2}	1.8664×10^{-2}	-9.9661×10^{-3}

Table II. Coefficients a_{mn} for Eq. (6).

m/n	n = 0	n = 1	n = 2	n = 3
0	-8.0155	1.8371	4.5233×10^{-2}	-5.9898×10^{-3}
1	3.6916×10^{-1}	-1.452×10^{-2}	-9.5873×10^{-4}	-5.2315×10^{-4}
2	-1.04307×10^{-2}	-3.0142×10^{-2}	7.1303×10^{-3}	-3.3802×10^{-4}
3	3.4718×10^{-3}	2.3603×10^{-3}	-6.8538×10^{-4}	3.9405×10^{-5}

$$R(\epsilon) = 2\left(\frac{0.01\ A}{-\frac{dE}{dX}(\epsilon = 0.01)}\right) + A\int_{0.01}^{\epsilon} \frac{d\epsilon'}{-\frac{dE}{dX}(\epsilon')}^{*} \tag{8}$$

for $0.01 \leq \epsilon \leq 10$ MeV/amu, or it is calculated from

$$R(\epsilon) = 2\left(\frac{0.01\ A}{-\frac{dE}{dX}(\epsilon = 0.01)}\right) + A\int_{0.01}^{10.0} \frac{d\epsilon'}{-\frac{dE}{dX}(\epsilon')} + \frac{A}{Z^2}\left[\lambda(\epsilon) - \lambda(10)\right]^{*} \tag{9}$$

for $\epsilon > 10$ MeV/amu, where λ is calculated from Eq. (6B).

B. Method for Z Greater Than Ten

The calculation of stopping power and range-energy data for high-Z ions has not been investigated thoroughly for as broad an energy region as is necessary for our purposes. Available information that is helpful to us is sparse.

1. Low-Energy Region ($137\ \beta \leq Z^{1/3}$)

In this energy region the ions are rapidly capturing electrons, thus losing effective charge and decreasing in their rate of energy deposition. The LET of the ions in this region is not large compared with that of ions in other energy regions. The average energy of ions at the Bragg peak is normally well above this region. Thus the stopping power of these ions is of relatively minor importance for biological purposes.

Considerable effort has been spent, however, to obtain good data in this region. There are two main reasons for this. First, there is some theory and some experimental fission-product data available in this region. Thus it is possible to provide fairly good results, and we seize the opportunity to be as complete as possible in this study. Second, we have relied heavily on these results for constructing stopping power in the medium-low and part of the medium-high energy regions. These latter energy regions are of great importance in radiological work, since they contain the region of maximum LET as well as most of the Bragg-peak energy. Thus the results of this low-energy region is indirectly of great importance.

*The first term of this expression is an estimate of the range of a 0.01 MeV/amu ion. We assume that the stopping power is directly proportional to $\epsilon^{1/2}$ below 0.01 MeV/amu.

There are two main stopping mechanisms operating in this region. One is the energy loss to electronic excitation and ionization of the stopping medium due to ion-electron collisions. This is called electronic stopping power. Lindhard and Scharff[3] used the Thomas-Fermi atomic model to find an expression for this effect. The other mechanism is the energy loss to the recoiling atom in the atom-atom elastic collisions between the ion and an atom of the stopping medium, i.e., the ion energy loss resulting in strictly a heating of the medium. (We neglect inelastic atom-atom collisions resulting in excitation of electronic levels of either the atom or the ion.) This is called nuclear stopping power. Recently Lindhard, Scharff, and Schiott[4] derived a universal curve for this effect, using the Thomas-Fermi model to determine the effects of screening. We find that this curve follows closely the function

$$-\frac{dE}{dX_n} = c_n \epsilon^{1/2} \exp\left[-45.2\,(c_{n1}\epsilon)^{0.277}\right], \qquad (10)$$

where $-(dE/dX)_n$ is the nuclear stopping power in units of MeV/g-cm^{-2}, ϵ is the energy in MeV/amu,

$$c_n = 4.14\times 10^6 \left(\frac{A}{A + A_t}\right)^{3/2} \left(\frac{ZZ_t}{A_t}\right)^{1/2} \frac{1}{\left(Z^{2/3} + Z_t^{2/3}\right)^{3/4}}, \qquad (11)$$

and

$$c_{n1} = \left(\frac{AA_t}{ZZ_t}\right)\left(\frac{1}{A + A_t}\right) \frac{1}{\left(Z^{2/3} + Z_t^{2/3}\right)^{1/2}}. \qquad (12)$$

At fission-product energies the electronic stopping power dominates the nuclear stopping power. Therefore, we choose to adjust the expression for the electronic stopping power so that the sum of the two stopping mechanisms corresponds with fission-product range values taken from references 5 through 11. The resulting expression for the electronic stopping power is

$$-\frac{dE}{dX_e} = c_e \epsilon^{1/2}, \qquad (13)$$

where

$$c_e = 7.4 \times 10^4 \frac{Z^{6/5} Z_t}{A_t \left(Z^{2/3} + Z_t^{2/3}\right)^{3/2}} . \qquad (14)$$

Thus for $137\,\beta \leq Z^{1/3}$ the stopping power is given by

$$-\frac{dE}{dX} = -\frac{dE}{dX_e} - \frac{dE}{dX_n}, \qquad (15)$$ *

where $-(dE/dX)_e$ and $-(dE/dX)_n$ are given by Eqs. (13) and (10), respectively.

2. High-Energy Region ($137\,\beta > 3Z$)

In the high-energy region, where the ion is assumed to be completely stripped of its orbital electrons, Eqs. (1) and (6) are used to get the ion stopping power. Thus

$$-\frac{dE}{dX}(\epsilon) = Z^2 \left[-\frac{dE}{dX}(\epsilon)\right]_p, \qquad (16)$$

where $(-dE/dX)_p$ is the Barkas and Berger proton stopping power given by Eq. (6).

3. Medium-High Energy Region ($9 < 137\,\beta \leq 3Z$)

This region is bounded on the high side by the energy at which the ion can be considered to be completely stripped of electrons. It is bounded on the low side by the lowest energy for which we believe the method described below can be reasonably used.

Our method uses charge-state data derived from range-energy data available for argon ions incident upon aluminum. These charge-state data are generalized to all ions for which $Z > 10$ and all stopping media as follows.

*When there are several atomic components in the stopping medium, this expression becomes

$$-\frac{dE}{dX} = \frac{1}{\rho} \sum_{i=1}^{N} \left\{ \rho_i\, c_{e_i}\, \epsilon^{1/2} + \rho_i\, c_{n_i}\, \epsilon^{1/2} \exp\left[-45.2\, (c_{n1_i}\, \epsilon)^{0.277}\right] \right\}$$

where c_{e_i}, c_{n_i}, and c_{n1_i} are the constants given by Eqs. (14), (11), and (12), respectively, evaluated for the ith atomic component.

Knipp and Teller,[12] on the basis of the Thomas-Fermi picture of the atom, derived a relationship between Z_{eff}/Z and $(v_e/v_i)(137\ \beta/Z^{2/3})$, where Z_{eff}/Z is the fractional ionization of the ion, β is the ratio of the ion velocity to the speed of light, and v_e/v_i is the ratio of the velocity of an electron in the ion's electron cloud to the velocity of the ion at which this electron is barely bound.

The factor (v_e/v_i) varies somewhat as a function of Z and Z_t, but here we assume it is a constant. Then Z_{eff}/Z should be a function of only $137\ \beta/Z^{2/3}$ when the electron cloud of the ion is populated to such an extent that the statistical nature of the Thomas-Fermi picture is appropriate. As the electron cloud is depleted, $137\ \beta/Z^{2/3}$ will no longer be the appropriate variable. In fact we expect the charge ratio Z_{eff}/Z to vary according to the variable $137\ \beta/Z$ for the limiting case of the one-electron atom. Thus we look for a function

$$\frac{Z_{eff}}{Z} = r(x), \tag{17}$$

where

$$x \equiv \frac{137\ \beta}{Z^g}, \tag{18}$$

with

$$\left.\begin{aligned} g &= 2/3 && \text{for } 137\ \beta \leq Z^{2/3}, \\ g &= \frac{137\ \beta + 4Z - 3Z^{2/3}}{6Z - 3Z^{2/3}} && \text{for } Z^{2/3} < 137\ \beta < 2Z, \\ \text{and} \quad g &= 1 && \text{for } 2Z \leq 137\ \beta \leq 3Z. \end{aligned}\right\} \tag{19}$$

The function $r(x)$ must satisfy the criteria:

1. $r(0) \doteq 0$,
2. $r(\infty)$ approaches 1 asymptotically,
3. For all Z and Z_t, $Z^2\ r^2\ (3)\ (dE/dX)$ and its first derivative are approximately continuous with the stopping power and its first derivative respectively at the low-energy end of the high energy region, (here dE/dX represents the proton stopping power),
4. For all Z and Z_t, $Z^2\ r^2(9/Z^g)\ (dE/dX)$ and its first derivative are approximately continuous with the stopping power and its first

derivative respectively at the high-energy end of the low-energy region,

5. $R(\epsilon) = \frac{A}{Z^2} \int_0^{\epsilon} \frac{d\epsilon^1}{r^2(x)\,(-dE/dX)_p}$ fits closely the known range-energy data for argon ions in aluminum. This range data is taken from estimates made by Northcliffe[13] which agree well with some experimental data.[14]

There is some question about which formulation of the proton stopping power to use in this energy region and thus in the search for r(x) as outlined above. The low-energy end of this region is outside the limits of validity for the Born approximation,[15] so that Bethe's theory is not valid. Yet the energy is too high for the classical approximation to be valid so that we cannot obtain accuracy with Bohr's theory. We feel it is best to search for a r(x) that satisfies the above criteria when Bethe's theory is used for the proton stopping power. When this is done, the function r(x) may not physically represent Z_{eff}/Z at the low-energy end of this region. However, the error in r(x) will complement the error in Bethe's theory, so that the final stopping power is fairly accurate.

A function that satisfies the above five criteria is

$$r(x) = 1 - \frac{\exp(-0.413X^{2.67})}{1.848} - \frac{0.848}{1.848(10.48X^{2.216} + 1)}, \qquad (20)$$

where $x = 137\,\beta/Z^g$, and g is defined in Eq. (19). The stopping power in this energy region is then given by

$$-\frac{dE}{dX} = Z^2 r^2 \left(-\frac{dE}{dX}\right)_p, \qquad (21)$$

where $-(dE/dX)_p$ is given by Eq. (5) for $\epsilon \leq 7$ MeV/amu and by Eq. (6) for $\epsilon > 7$ MeV/amu.

4. <u>Medium-Low Energy Region ($Z^{1/3} < 137\,\beta \leq 9$)</u>

This is a narrow region connecting the variable upper limit of the low-energy region with the fixed lower limit of the medium-high energy region. There is no available data in this region which is satisfactory for estimating the stopping power of ions with $Z > 10$. However since this region is so narrow, a simple cubic polynomial, matching slope and magnitude of the stopping power at both boundaries, provides the stopping power within the region very adequately.

We know that stopping power tends to depend upon energy in a

logarithmic fashion. Thus it is to be expected that a polynomial fit of the stopping power should contain $\ln\epsilon$ as the variable. Thus we choose a cubic polynomial of the form

$$\ln\left(-\frac{dE}{dX}\right) = a_1 + a_2 \ln\epsilon + a_3 (\ln\epsilon)^2 + a_4 (\ln\epsilon)^3, \tag{22}$$

which is completely determined by the magnitude and first derivative of the stopping power at the upper and lower boundaries of this region.

5. Range Calculation

The range of an ion of ϵ MeV/amu for ϵ in the high-energy region is calculated from

$$R(\epsilon) = A \int_0^{\epsilon_1} \frac{d\epsilon}{-\frac{dE}{dX}_L} + A \int_{\epsilon_1}^{\epsilon_2} \frac{d\epsilon}{-\frac{dE}{dX}_{ML}} + A \int_{\epsilon_2}^{\epsilon_3} \frac{d\epsilon}{-\frac{dE}{dX}_{MH}}$$

$$+ \frac{A}{Z^2} [\lambda(\epsilon) - \lambda(\epsilon_3)], \tag{23}$$

where $(-dE/dX)_L$, $(-dE/dX)_{ML}$, $(-dE/dX)_{MH}$, and λ are given in Eqs. (15), (22), (21), and (6B) respectively, ϵ_1 and ϵ_2 are respectively the lower and upper limits of the medium-low energy region, and ϵ_3 is the lower limit of the high-energy region. For ϵ in the medium-high-energy region, the last term of Eq. (23) is deleted. If ϵ is in the medium-low-energy region, the last two terms are deleted, and if ϵ is in the low-energy region, only the first term is used.

III. DISCUSSION OF METHOD

A. Z Less Than Ten

1. Energies Less Than 10 MeV/amu

For $Z \leq 10$ and $\epsilon \leq 10$ MeV/amu considerable experimental data are available. Northcliffe[1] has developed a graphical technique to smooth these data and extend them to some ions and stopping materials for which there is no experimental data. Where there are data points from more than one investigator, a spread in the points of 20% is not uncommon. In some cases the spread is 50%. The total spread in uncertainty (i.e., twice the absolute uncertainty) for the data points quoted by the investigators varies from about 5 to 30%.

Northcliffe's graphical technique is designed to follow closely the data points he believes to be the most reliable. We believe it is reasonable to assume the smooth curve generated by Northcliffe to be within 5 to 10% of the correct value for $0.1 \leq \epsilon \leq 5$ MeV/amu. Above 5 MeV/amu his curve should be very accurate (within a couple percent) because charge exchange becomes less significant. Below 0.1 MeV/amu the few experimental data points were obtained under very difficult conditions. Thus they are possibly less accurate than those obtained at higher energies. Likewise we are less certain of the accuracy of Northcliffe's smooth curve for $\epsilon < 0.1$ MeV/amu.

The results of the calculation presented in this paper for $Z \leq 10$ and $\epsilon \leq 10$ MeV/amu differ from Northcliffe's graphical technique by less than the uncertainty we attribute to his method. We by no means claim that our calculation is more accurate than the results by Northcliffe. We claim rather that where our results differ from his, the effort required to bring about closer agreement is unjustified. In Figs. 2 through 6 we have compared our results with points from Northcliffe's graphical technique. In these figures we see that the agreement for $\epsilon > 0.1$ MeV/amu is quite good. For aluminum and silver as the stopping medium, agreement is good over the entire energy range. Where the disagreement is greatest, it approaches 20%.

Our method is normalized to Northcliffe's results for aluminum as the stopping material, since we feel that the aluminum data are the most reliable. Stopping power values estimated by our method for $\epsilon \leq 10$ MeV/amu and $Z \leq 10$ seem to be slightly larger for most other stopping materials than the values estimated by Northcliffe.

2. Energy Greater Than 10 MeV/amu

For $Z \leq 10$ and $\epsilon > 10$ MeV/amu, stopping power and range are calculated by using Eqs. (7) and (9) respectively.

Given that the ions under consideration are completely ionized, the stopping power calculated by Eq. (7) is as accurate as the polynomial of Barkas and Berger [Eq. (6)]. Barkas and Berger[2] have determined that the root-mean-square percentage deviation of this polynomial from 600 points calculated with their modified Bethe theory is 0.6% for λ

and 1.3% for the stopping power. The maximum error for the range is 2.8%.

3. Range for $Z \leq 10$

The range given by Eq. (9) is consistent with the stopping power evaluated above. The first term of Eq. (9) gives the range for a 0.01 MeV/amu ion, if we assume that the stopping power varies as $\epsilon^{1/2}$ below 0.01 MeV/amu. We perform the integration indicated in the second term, assuming that the stopping power maps a straight line on log-log graph paper between the points taken from Fig. 1.

B. Z Greater Than Ten

1. Low-Energy Region

The stopping power for these ions is given in Eq. (15). It is based upon a theory developed by Lindhard et al.[3,4] from the Fermi-Thomas model of the atom. In developing their theory, Lindhard et al. treat separately the effect of elastic collisions between the ion and the Coulomb field of the nuclei in the stopping material, and the effect of inelastic collisions between the ion and the atomic electrons in the stopping material. This separation may result in systematic overestimation of the stopping power, according to Lindhard. Lindhard also warns that the validity of this theory is uncertain for $\epsilon \leq 10^{-2}$ MeV/amu, since the Fermi-Thomas treatment of the atom is a crude approximation when the ion and atom do not come close to each other.

We appreciate the critical appraisal Lindhard affords his own work, but we hasten to draw attention to the agreement between Eq. (15) and the experimental fission-product ranges demonstrated in Table III. The energies and experimental ranges for the fission products presented in Table III are taken from references 5 through 11.

2. High-Energy Region

For ions in this region, the stopping power is given by Eq. (16). This equation is the same as Eq. (7) which was discussed in Sec. IIIA2. The same Barkas-Berger polynomial is used here.

Bethe's theory, which is the basis of the results of Barkas and Berger,[2] is not valid for either large Z (ion atomic number) or large

Table III. Comparison of ranges calculated by program with experimental fission-product ranges.

Ion	Stopping Material	Estimated energy (MeV/amu)	Range (mg/cm^2)	
			Experimental	Calculated
$^{89}_{38}Sr$	Al	1.12	4.09	4.16
$^{115}_{48}Cd$	Al	0.613	3.32	3.18
$^{140}_{56}Ba$	Al	0.489	2.98	3.07
$^{144}_{58}Ce$	Al	0.437	2.76	2.88
$^{89}_{38}Sr$	U	1.12	11.55	12.83
$^{109}_{46}Pd$	U	0.816	10.14	10.88
$^{115}_{48}Cd$	U	0.613	9.52	9.28
$^{140}_{56}Ba$	U	0.489	8.74	8.49
$^{144}_{58}Ce$	U	0.437	8.37	7.86

Z_t (atomic number of stopping material). However, the addition of shell corrections by Barkas and Berger extends Bethe's theory to high Z_t. The restriction on Z is due to the fact that the Born approximation was used by Bethe. This approximation is valid if the velocity of the ion is significantly greater than the K-shell velocity of the ion.[15] This condition is certainly satisfied for this high-energy region. We therefore conclude that the Barkas-Berger polynomial is valid for our present purpose and that the stopping power we seek is satisfactorily given in Eq. (16).

3. Medium-High-Energy Region

The ability of Eq. (21) to give accurate stopping power depends primarily upon two assumptions. The first assumption is that a function r(x) exists [see Eqs. (17) through (20)]. If v_e/v_i is a constant (see Sec. IIB3), then the Thomas-Fermi atomic model is compatible with this assumption. However, for the high end of this energy region, the Thomas-Fermi model is not valid, since the ion is nearly completely stripped of electrons, so that a statistical model is not applicable. For two reasons we feel that the error introduced here is quite small. First, by allowing the variation in g (see Fig. 19), we have modified the behavior of the function r(x) so that it can reflect the proper divergence from the Thomas-Fermi model. Second, the effect of r(x) upon the stopping power at the high-energy end of this region is very small (i.e., r approaches 1.0) so that the final answer is not very sensitive to the model used.

Before the Thomas-Fermi model can give any assurance that the function r(x) does exist, we must assume that v_e/v_i is a constant. Brunnings, Knipp, and Teller[16] investigated this ratio. Using the Thomas-Fermi model, they made the two extreme assumptions--first, that v_e is the velocity of the least tightly bound electron on the ion, and second, that v_e is the velocity of the outermost electron. For the first assumption, the empirically indicated values of v_e/v_i are, for Z = 10,

$$\frac{v_e}{v_i} \approx 1.2,$$

and for Z = 55

$$\frac{v_e}{v_i} \approx 1.8.$$

The second assumption gives, for Z = 6,

$$\frac{v_e}{v_i} \approx 0.6,$$

and for Z = 55,

$$\frac{v_e}{v_i} \approx 0.35.$$

These results show that v_e/v_i is undoubtedly not a constant with Z. However, since these two assumptions give variations in opposite directions, assuming v_e/v_i to be constant seems appropriate.

The second assumption necessary for the validity of Eq. (21) is that our choice of r(x) cancels the errors in Bethe's theory when it is inappropriately used in this energy region. The use of the Born approximation by Bethe limits the appropriate use of his theory to energies where the inequalities[15]

$$u^2 \ll v^2 \quad \text{or} \quad Z_{eff} \ll Z_t$$

and

$$Z_{eff} \ll 137\,\beta$$

are satisfied. Here u is the orbital velocity of electrons in the stopping medium, v is the ion velocity, Z_{eff} is the effective charge on the ion, Z_t is the nuclear charge in the stopping medium, and $\beta = v/c$. These inequalities are not satisfied, for instance, for argon ions in aluminum when the ion energy is less than about 10 MeV/amu. One might anticipate trouble here since the lower limit of this energy region is 2 MeV/amu. In this case, however, Eq. (21) gives the right answer because the function r(x) is found in the first place by dividing empirically indicated stopping powers of Ar in Al by stopping powers calculated from Bethe's theory, with complete ionization of the ion assumed. Thus, in the case of Ar in Al, r(x) is not the correct value of Z_{eff}/Z for $\epsilon < 10$ MeV/amu, nor does Bethe's theory give the correct stopping power;

however the product of the two cancel each others errors to give the correct stopping power.

Another factor affecting r(x) which is neglected is the variation in r(x) as a function of the different stopping media. In stopping media with higher electron densities, the time interval between ion-electron collisions is shorter. Thus the electronic levels of the ion excited by one collision will have less opportunity to relax before the next collision. The probability of removing an electron from the ion is greater for these higher-density media because the electrons are maintained in more highly excited states. This leads us to suspect that r(x) should be larger for stopping media with greater electron densities. In the work presented here, we have neglected this effect. For high-Z ions and high-Z_t media, we have adjusted r(x) at the lower boundary of this medium-high energy region to be large enough to avoid any discontinuity with the upper boundary of the low-energy region. We find, as expected, that for high-Z ions and low Z_t media (i.e., low electron density), the stopping power is slightly too large at the lower boundary of this energy region to match well the stopping power at the upper boundary of the low-energy region. We feel that errors due to this effect are small compared to the uncertainty of the total calculation, however.

We believe that by choosing r(x) to satisfy the five criteria in Sec. IIB3, we should obtain valid results from Eq. (21) for energies near the upper and lower limits of this region. For very heavy ions, the above inequalities are not satisfied except for very high energy. In this case the accuracy of Bethe's theory and the variation in v_e/v_i are not certain. We do not expect the error in Eq. (21) for very heavy ions to be large, but for energies away from the upper and lower limits of this region, experimental data from the Omnitron will be necessary before we can be confident.

4. Medium-Low Energy Region

The upper limit of this region is 2 MeV/amu. The lower limit ranges from 0.1 to 0.5 MeV/amu as Z ranges from 10 to 92 respectively. Thus this energy region is very narrow. Using Eq. (22) and matching

the slope and magnitude of the stopping power at both boundaries we cannot expect the error within the region to differ significantly from that at the boundaries.

5. The Range Calculation

The range is given by Eq. (23). The integrals are solved numerically by Simpson's rule. The number of intervals into which the domain of integration is divided is doubled for each successive trial, and the convergence criterion is set such that the value of the integral is given by the second of two consecutive trials that differ by less than 0.5%. Thus the range calculation is consistent with the stopping-power calculation discussed above. The accuracy of the range calculation is essentially the same as that of the stopping-power calculation.

V. RESULTS

A computer program has been written in CHIPPEWA FORTRAN which computes range-energy and stopping-power data, using the methods discussed above. The program is also available upon request in FORTRAN IV computer language.

This program has been used to obtain data to be presented here for several selected ions and stopping media. The ions chosen were hydrogen, helium-4, carbon-12, neon-20, argon-40, krypton-84, xenon-131, and uranium-238. Data are presented for each of these ions incident upon water, aluminum, copper, silver, lead, and uranium.

In Figs. 7 through 12, stopping power has been plotted as a function of energy. One of the conspicuous features of these curves is the difference in behavior in the low-energy region between the ions for $Z > 10$ and for $Z \leq 10$. This reflects the fact that a completely different method is used to calculate the stopping power in these two cases. For $Z > 10$, Eq. (15) is used. The increasing contribution of the nuclear stopping-power term as Z increases and ϵ decreases causes the slope of the curves to decrease under these conditions. Lindhard et al. states that the separation of the two terms in Eq. (15) may lead to a systematic overestimation of the stopping power in this low-energy region.[4]

Northcliffe's graphical technique, a modified version of which is used for $Z \leq 10$, does not consider this increased energy loss to heating the stopping medium at these low energies.[1] Thus this effect may be overestimated for argon ions and underestimated for neon ions, leading to a discontinuity in the systematic change of behavior across the $Z = 10$ boundary. However, the actual difference in magnitude of the stopping power as calculated by these two methods is not alarming. This can be seen in Fig. 13, where stopping power is plotted as a function of energy for neon ions in aluminum. The curve showing a decreasing slope at very low energy is calculated by the method normally used only for $Z > 10$. The other curve is calculated by the method used for $Z \leq 10$. Another conspicuous feature of Figs. 7 through 12 is the slight change in slope of the krypton ion curve at 150 MeV/amu. For krypton this energy corresponds to $137\ \beta = 2Z$, which is the point at which the function g [see Eq. (19)] changes slope and is given the constant value 1.0. This artificial behavior of the function g gives an artificial behavior to this stopping-power curve. (Similar behavior of the other curves for $Z > 10$ is not as conspicuous.) However, the fluctuation in magnitude of the stopping power due to this artificial behavior is insignificant.

In Sec. IIIB3 we discussed the possibility that our technique for calculating stopping power near 2 MeV/amu for ions of high Z and stopping media of low Z_t would yield results that are slightly too large. This effect can be seen in Fig. 7 for uranium ions in water. The cubic polynomial in the medium-low energy range which connects the 2- and 0.6-MeV/amu points obscures this effect somewhat. However, the effect appears to be quite small.

The very slight bump at 7 MeV/amu which is visible in Figs. 8 through 11 is due to the fact that Eqs. (5) and (6) do not match perfectly at 7 MeV/amu. At this energy we stop using Eq. (5) with Eq. (21) and begin using Eq. (6) to calculate the proton stopping power. This bump is a curiosity, but otherwise completely insignificant.

In Figs. 14 through 19 the stopping power is plotted as a function of ion residual range. The symbols on each curve mark points

corresponding to various energies. From Fig. 14, for instance, we can see that a 5 MeV/amu ^{20}Ne ion in water has a LET value of 7500 MeV/g-cm^{-2} and a range of 98 microns (about 10 mammalian cell diameters).

All of the interesting features of the previous set of curves (Figs. 7 through 13) are also present in this set. The reader is referred to the discussion above, as it will not be repeated here.

None of the previous figures, however, show the neon-carbon or xenon-uranium crossovers that we see in Fig. 14. A possible explanation is that these crossovers represent an inaccuracy in the program. Although this is a definite possibility (the curves cross over by only 10% in energy regions of relatively low confidence), we hasten to propose alternative possibilities. Velocity or energy is the natural variable of stopping power, not residual range. Thus apparent bizarre behavior for these curves may not, upon closer examination, be bizarre at all.

An alternative possibility is presented intuitively as follows. We expect the charge state of the ion to vary according to its velocity. Yet the energy varies also according to the mass. As we go to heavier ions, the mass increases faster than the nuclear charge. Thus the mass may increase faster than the effective charge, and the energy (i.e., range) may increase faster than the stopping power. Referring again to Fig. 14, as we go to heavier ions, we might therefore expect the curves to shift to the right faster than they shift vertically, ultimately crossing over, or at least contributing to a crossover. Unfortunately the credibility of this argument is lessened somewhat by the fact that the stopping power increases as the square of the effective charge on the ion.

Another alternative is expressed geometrically. For this argument the A/Z ratio of the ions may remain constant. Consider the two hypothetical stopping-power curves as a function of energy in Fig. 20. Curve A represents a stopping-power curve for a heavier ion than does curve B. At low energy the contribution to the total stopping power by the nuclear stopping-power component is therefore greater for curve A than for curve B, as we can see from the figure. Let area A_1 equal

area B_1, implying that the ranges for the two ions are equal when their stopping powers are $S(A_1)$ and $S(B_1)$ respectively.* Let this range be represented by R_1. Similarly let area A_2 equal area B_2, and area A_3 equal area B_3. The corresponding ranges are assigned the values R_2 and R_3 respectively. From Fig. 20 we see that for range R_1, $S(A_1)$ is greater than $S(B_1)$; for range R_2, $S(A_2)$ is less than $S(B_2)$; and for range R_3, $S(A_3)$ is greater than $S(B_3)$. For these two ions, therefore, the stopping-power curves as a function of residual range cross over in a manner similar to the crossover of the xenon and uranium curves in Fig. 14.

Our thoughts on the crossover that appears in Fig. 14 may be summarized as follows. The magnitude of the crossovers is less than the certainty we place upon the stopping-power calculation at the places where the crossovers occur. Thus the crossovers may not represent physical reality. However, crossovers of this kind may be a physical reality under certain circumstances.

In Figs. 21 through 26 the energy is plotted as a function of residual range. The discontinuity in the systematic change of behavior across the Z = 10 boundary, as discussed above, is apparent in these curves below 0.1 MeV/amu.

---

*Actually the ratio of area A_1 to area B_1 should equal the ratio of the atomic weight of ion B to the atomic weight of ion A in order for the ion ranges mentioned to be equal. Including this fact would complicate, but not change in substance, the argument. Therefore, for present purposes, we assume the ratio of the atomic weights to be negligibly different from 1.0.

V. ACKNOWLEDGMENT

This work was done under the auspices of the U. S. Atomic Energy Commission, and was partially completed under its Special Fellowship Program in Health Physics, which is administered by the Oak Ridge Associated Universities.

VI. BIBLIOGRAPHY

1. L. C. Northcliffe, "Passage of Heavy Ions Through Matter," Ann. Rev. Nucl. Sci. 13, 67 (1963).
2. W. H. Barkas and M. J. Berger, "Tables of Energy Losses and Ranges of Heavy Charged Particles," in Studies in Penetration of Charged Particles in Matter (National Academy of Sciences—National Research Council, Washington, D. C., 1964), p. 103.
3. J. Lindhard and M. Scharff, "Energy Dissipation by Ions in the KeV Region," Phys. Rev. 124, 128 (1961).
4. J. Lindhard, M. Scharff, and H. E. Schiott, "Range Concepts and Heavy Ion Ranges (Notes on Atomic Collisions, II)," Kgl. Danske Videnskab. Selskab, Mat.-Fys. Medd. 33, 14 (1963).
5. E. K. Hyde, "Kinetic Energy of Fission Fragments," in The Nuclear Properties of the Heavy Elements, III-Fission Phenomena (Prentice-Hall, Englewood Cliffs, New Jersey, 1964), p. 157.
6. J. C. C. Milton and J. S. Fraser, "Time-of-Flight Fission Studies on U^{233}, U^{235}, and Pu^{239}," Can. J. Phys. 40, 1626 (1962).
7. F. Suzor, "Tracks in Various Materials of Uranium Fission Fragments," Ann Phys. (Paris) (Ser. 12) 4, 269 (1949). In French.
8. N. K. Aras, "Range of Fragments from Thermal Fission of U^{235}," Ph. D. thesis, Mass. Inst. Tech., 1964.
9. J. M. Alexander and M. F. Gazdik, "Recoil Properties of Fission Products," Phys. Rev. 120, 874 (1960).
10. B. Finkle, E. J. Hoagland, S. Katcoff, and N. Sugarman, "Range of Fission-Recoil Fragments of Known Mass Numbers," papers 45 and 46 in Radiochemical Studies-The Fission Products, NNES IV Vol. 9 (McGraw-Hill, New York, 1951).
11. J. B. Niday, "Radiochemical Study of the Ranges in Metallic Uranium of the Fragments From Thermal Neutron Fission," Phys. Rev. 121, 1471 (1961).
12. J. Knipp and E. Teller, "On the Energy Loss of Heavy Ions," Phys. Rev. 59, 659 (1941).

13. L. C. Northcliffe, "Passage of Heavy Ions Through Matter II. Range-Energy Curves," in Studies in Penetration of Charged Particles in Matter (National Academy of Sciences—National Research Council, Washington, D. C., 1964), p. 173.

14. John Lyman, Lawrence Radiation Laboratory, Berkeley, California, private communication.

15. N. F. Mott and H. S. W. Massey, The Theory of Atomic Collisions (Oxford University Press, London, 1965).

16. J. H. M. Brunings, J. K. Knipp, and E. Teller, "On The Momentum Loss of Heavy Ions," Phys. Rev. 60, 657 (1941).

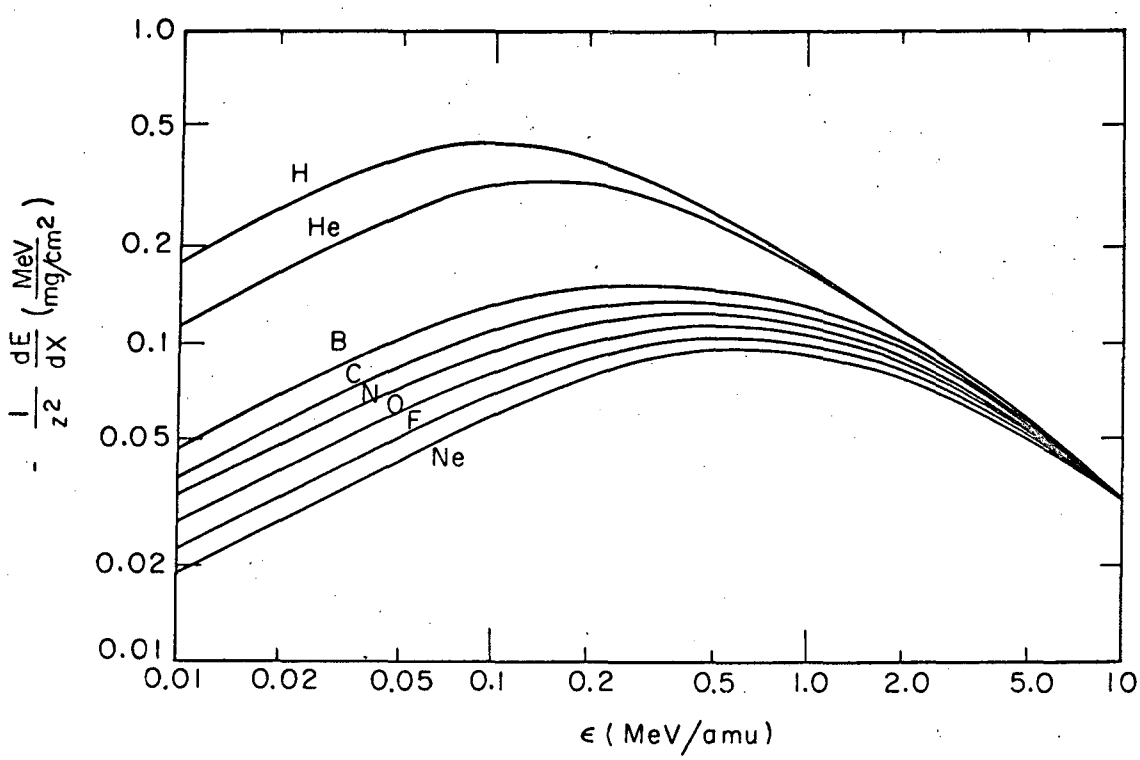

XBL672 — 671

Fig. 1. Smoothed stopping-power curves for various ions in aluminum. These data from Northcliffe[1] are the basis of the stopping-power calculation for $Z \leq 10$ and $\epsilon < 10$ MeV/amu.

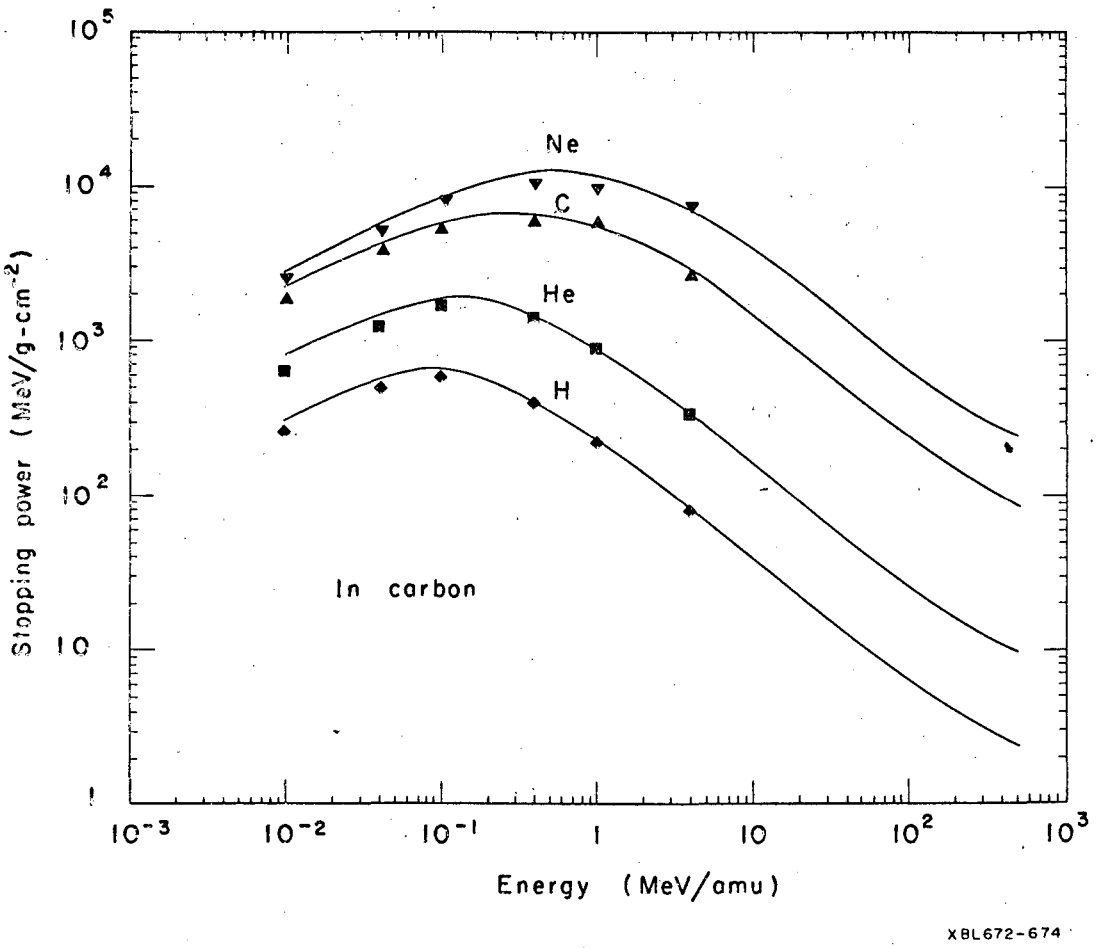

Fig. 2. Stopping power for various ions in carbon. The smooth curves are calculated by the computer program. The points are taken from Northcliffe's smoothed experimental data.[1]

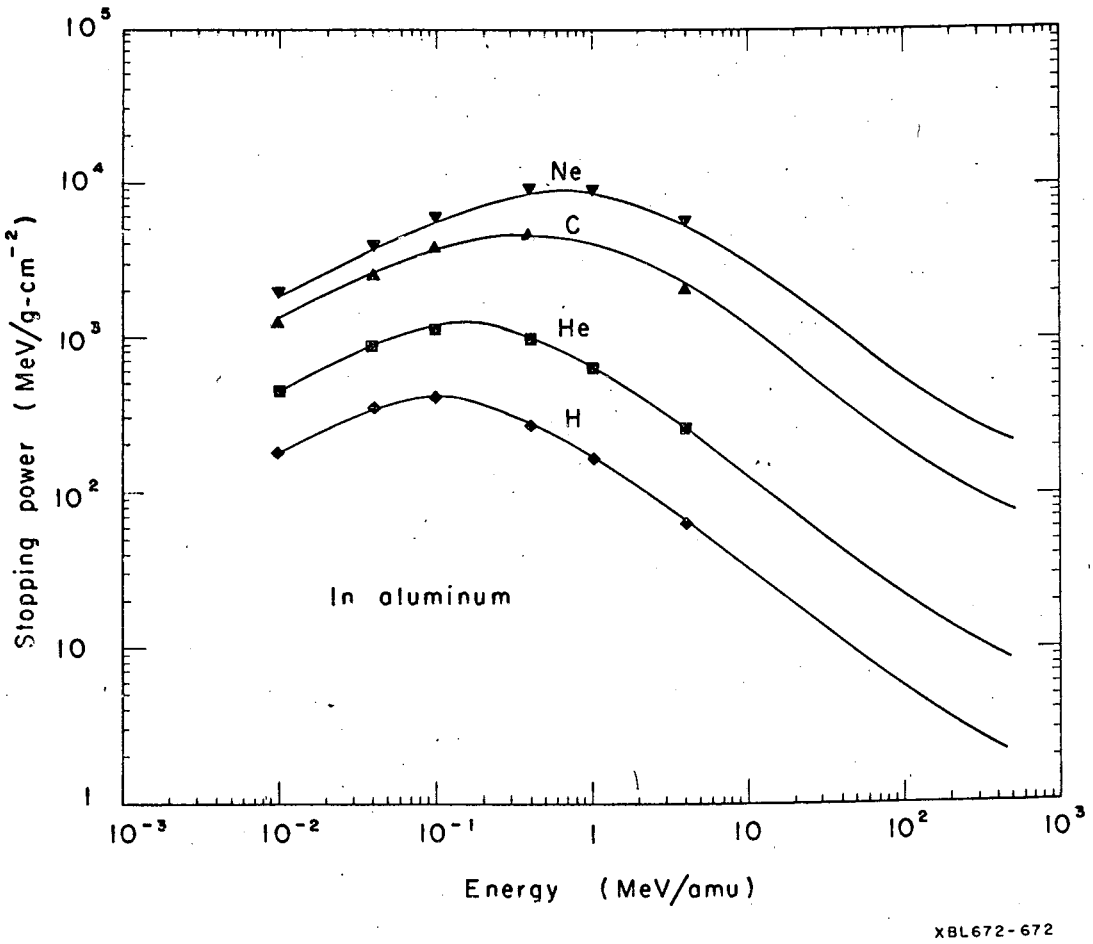

Fig. 3. Stopping-power for various ions in aluminum. The smooth curves are calculated by the computer program. The points are taken from Northcliffe's smoothed experimental data.[1]

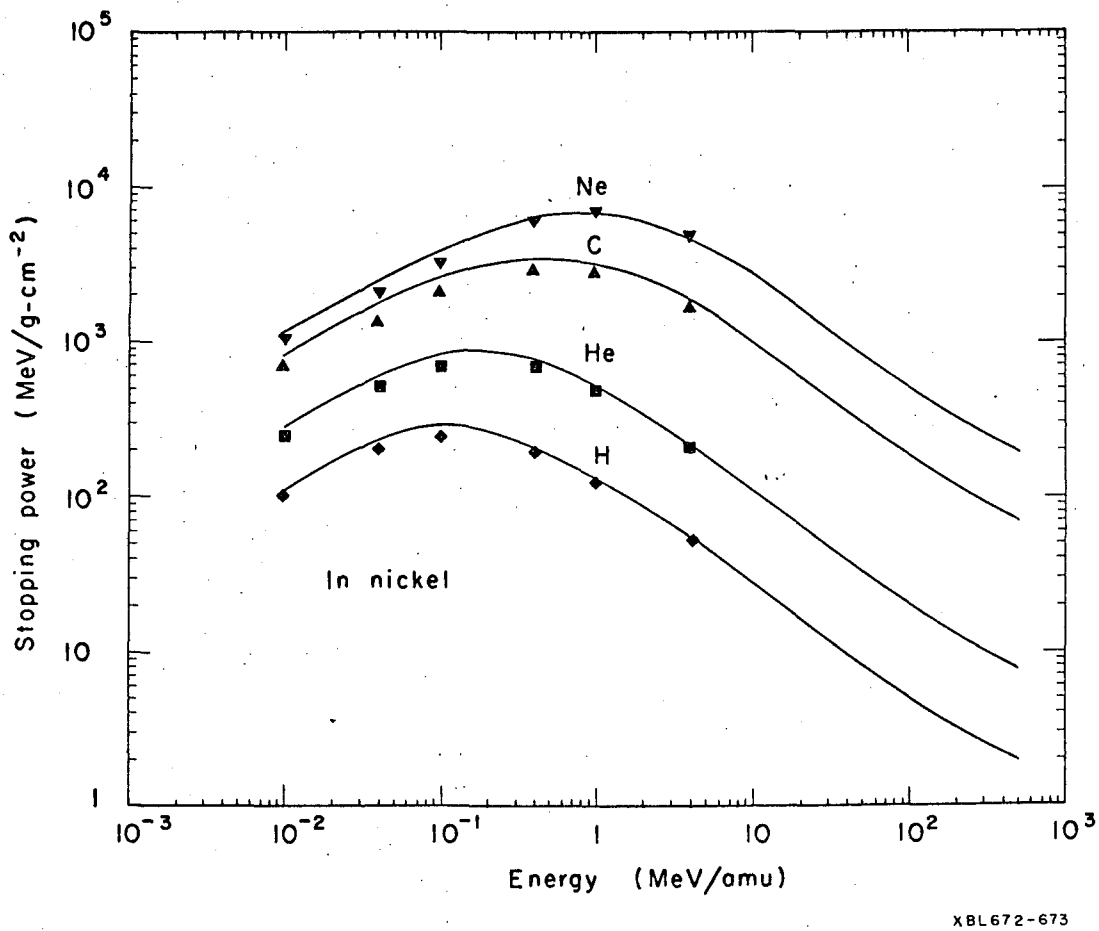

Fig. 4. Stopping-power for various ions in nickel. The smooth curves are calculated by the computer program. The points are taken from Northcliffe's smoothed experimental data.[1]

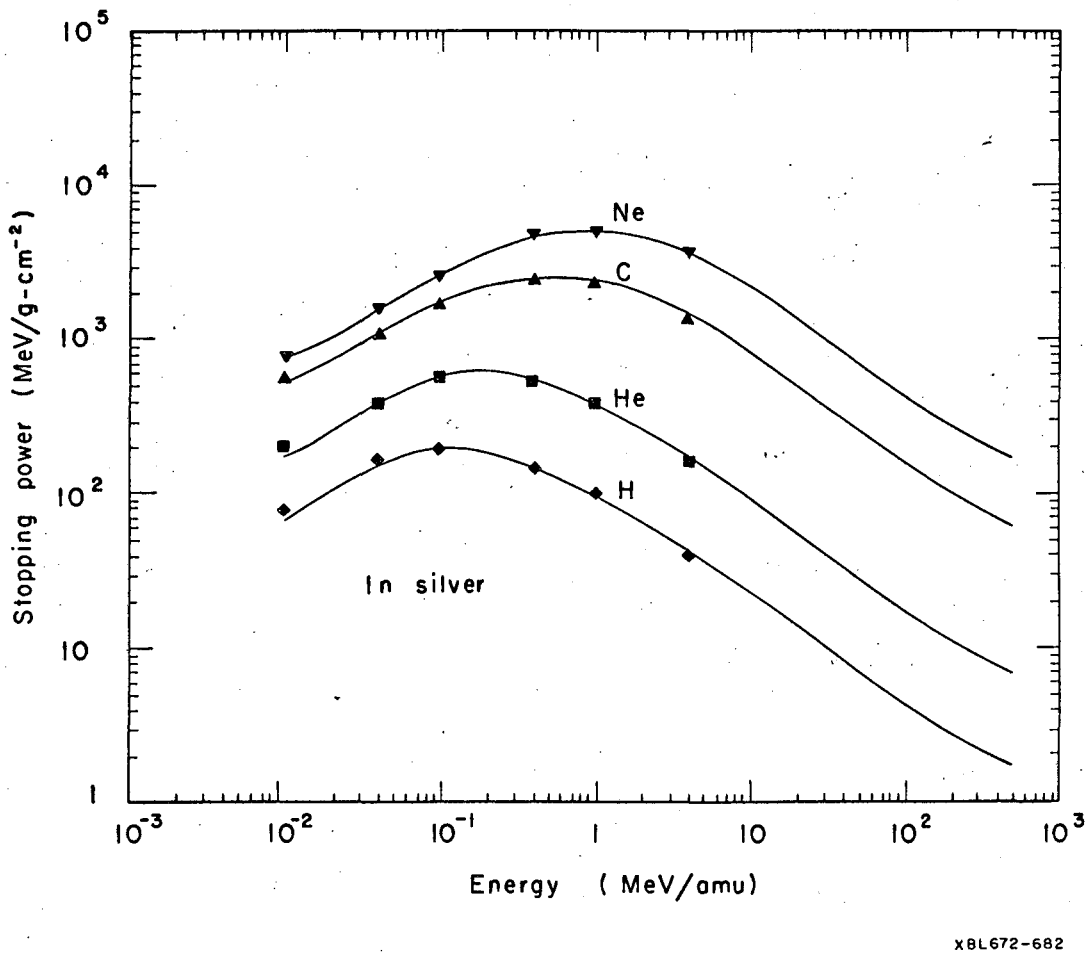

Fig. 5. Stopping-power for various ions in silver. The smooth curves are calculated by the computer program. The points are taken from Northcliffe's smoothed experimental data.[1]

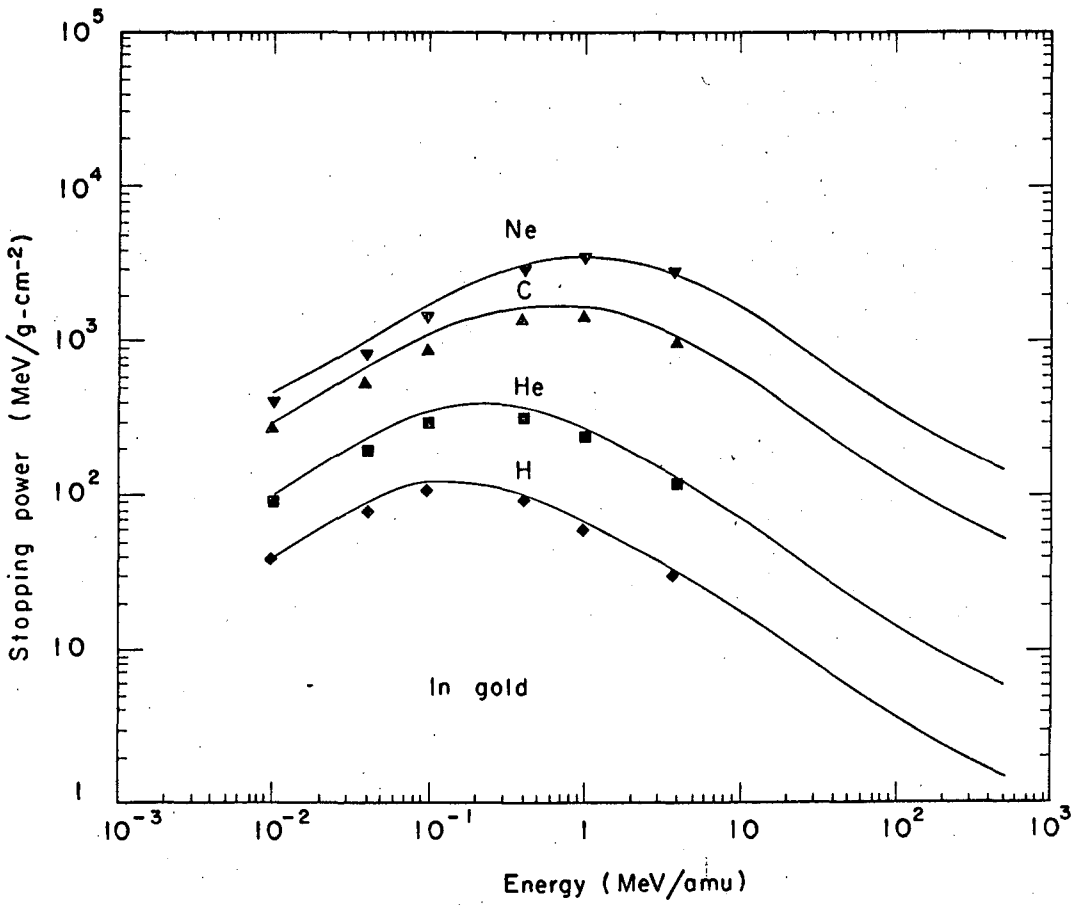

Fig. 6. Stopping-power for various ions in gold. The smooth curves are calculated by the computer program. The points are taken from Northcliffe's smoothed experimental data.[1]

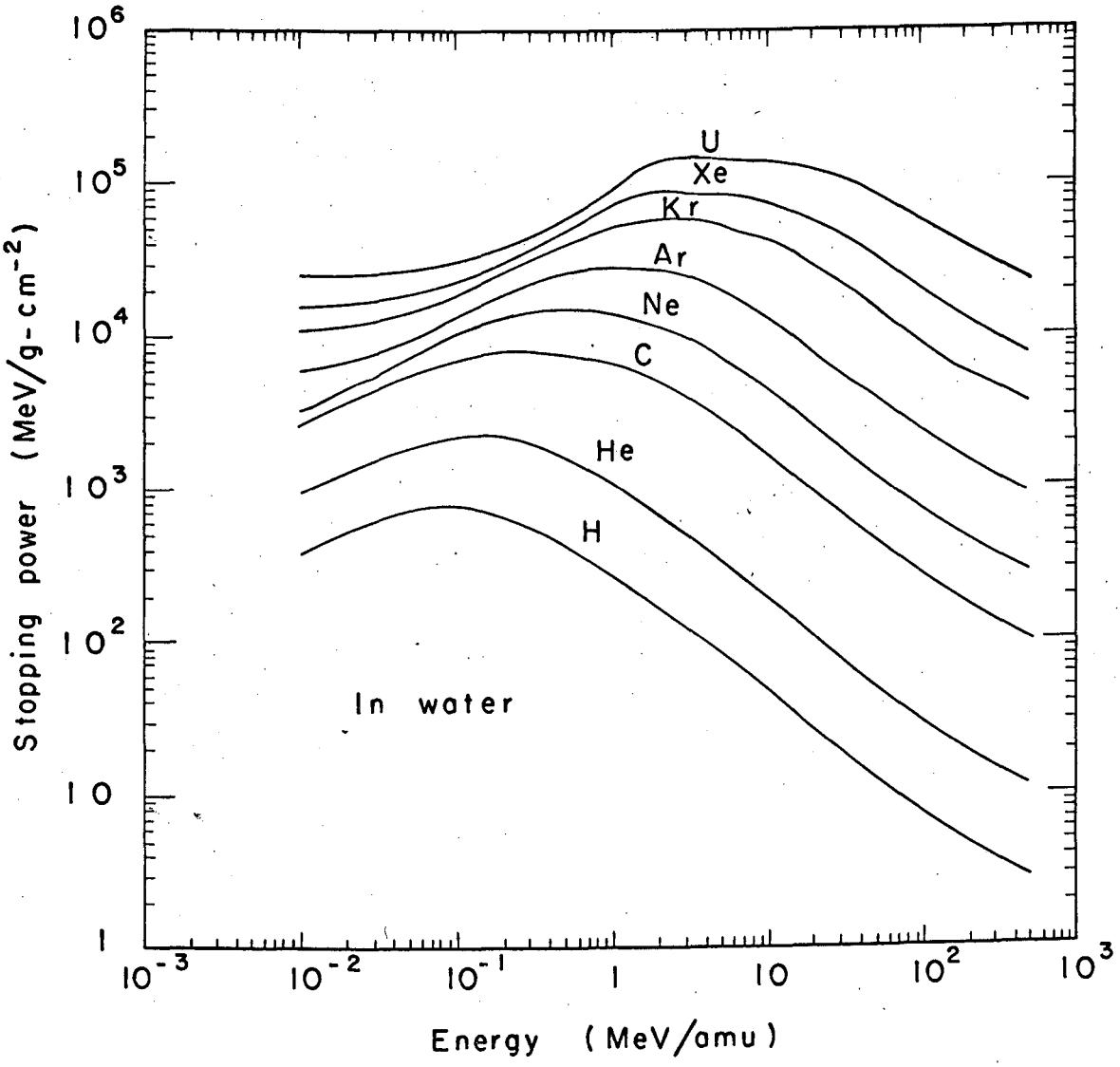

XBL672-684

Fig. 7. Stopping-power curves as a function of energy for various ions in water as calculated by the computer program. The small discontinuity in slope for Kr at 150 MeV/amu is at 137 $\beta = 2Z$, where the function g becomes 1.0 [see Eq. (19)]. The stopping power for U at the lower boundary of the medium-high energy region (2 MeV/amu) is slightly too large to match well the stopping power at the upper boundary of the low-energy region (0.6 MeV/amu), as discussed in Sec. IIIB3.

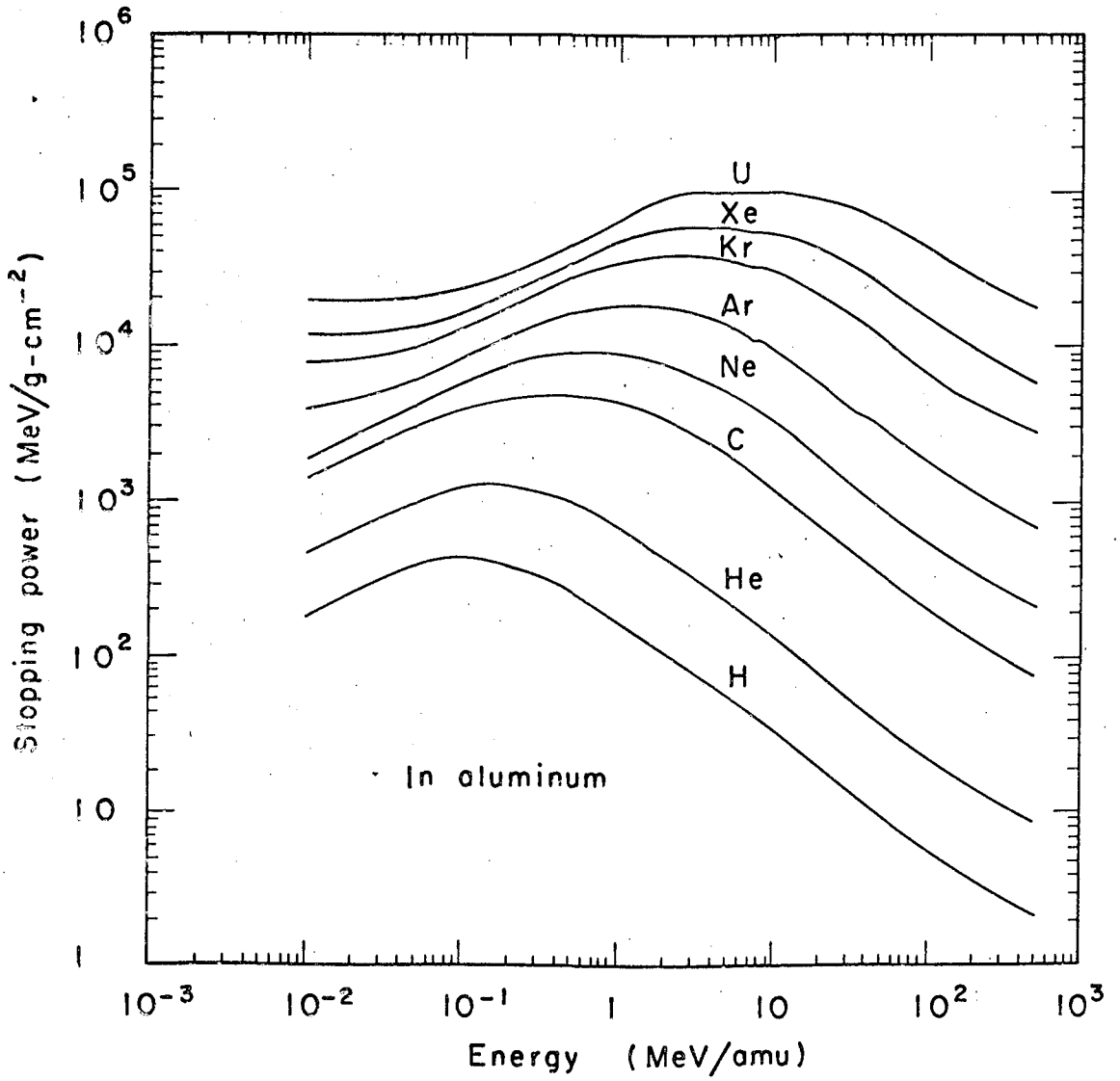

XBL672-685

Fig. 8. Stopping power curves as a function of energy for various ions in aluminum as calculated by the computer program. The small discontinuity in slope for Kr at 150 MeV/amu is at 137 $\beta = 2Z$, where g becomes 1.0 [see Eq. (19)]. The slight discontinuity at 7 MeV/amu for ions with $Z > 10$ is due to the fact that Eqs. (5) and (6) as employed by Eq. (21) do not match perfectly here.

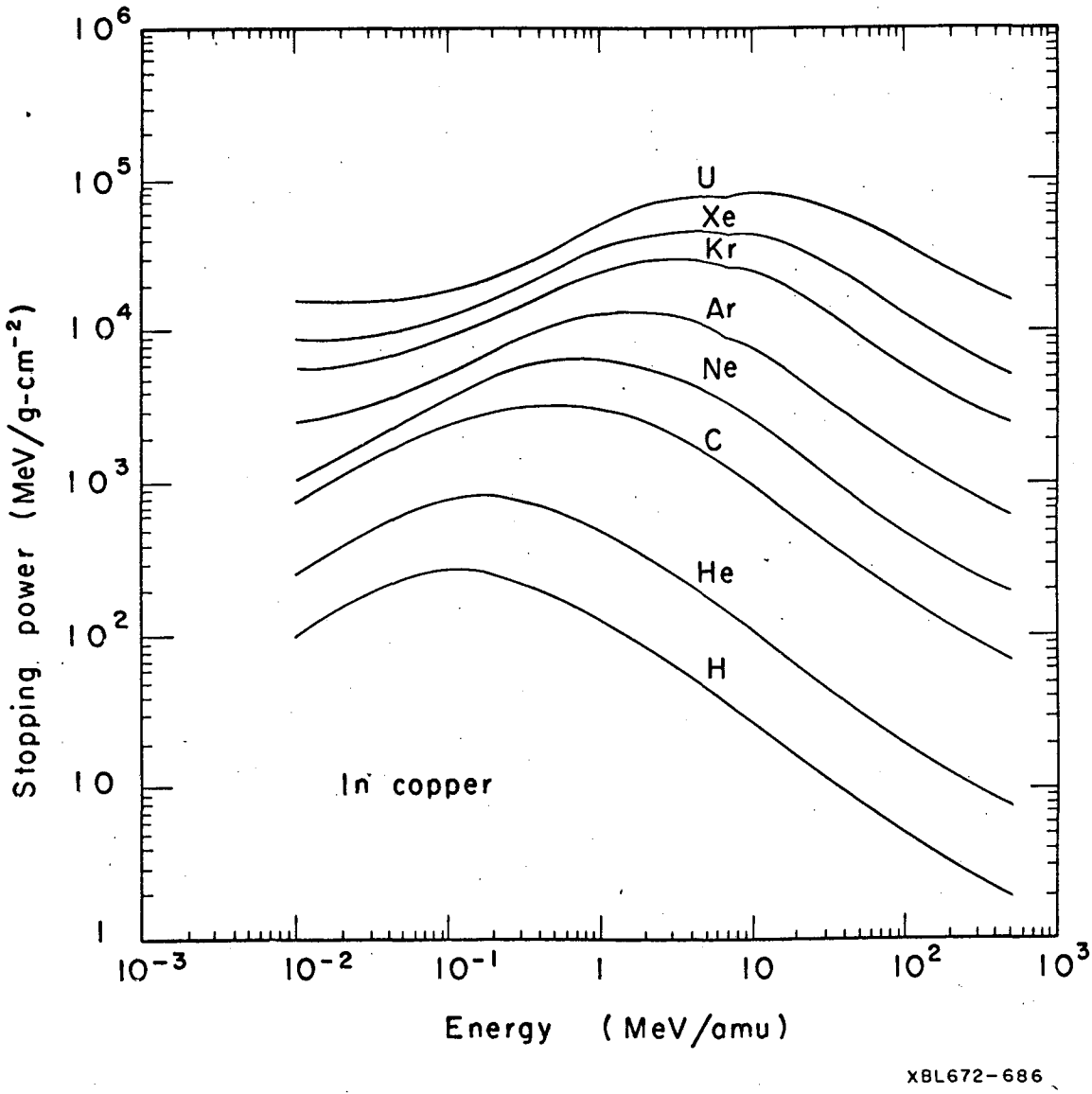

Fig. 9. Stopping-power curves as a function of energy for various ions in copper as calculated by the computer program. The small discontinuity in slope for Kr at 150 MeV/amu is at 137 $\beta = 2Z$, where g becomes 1.0 [see Eq. (19)]. The slight discontinuity at 7 MeV/amu for ions with $Z > 10$ is due to the fact that Eqs. (5) and (6) as employed by Eq. (21) do not match perfectly here.

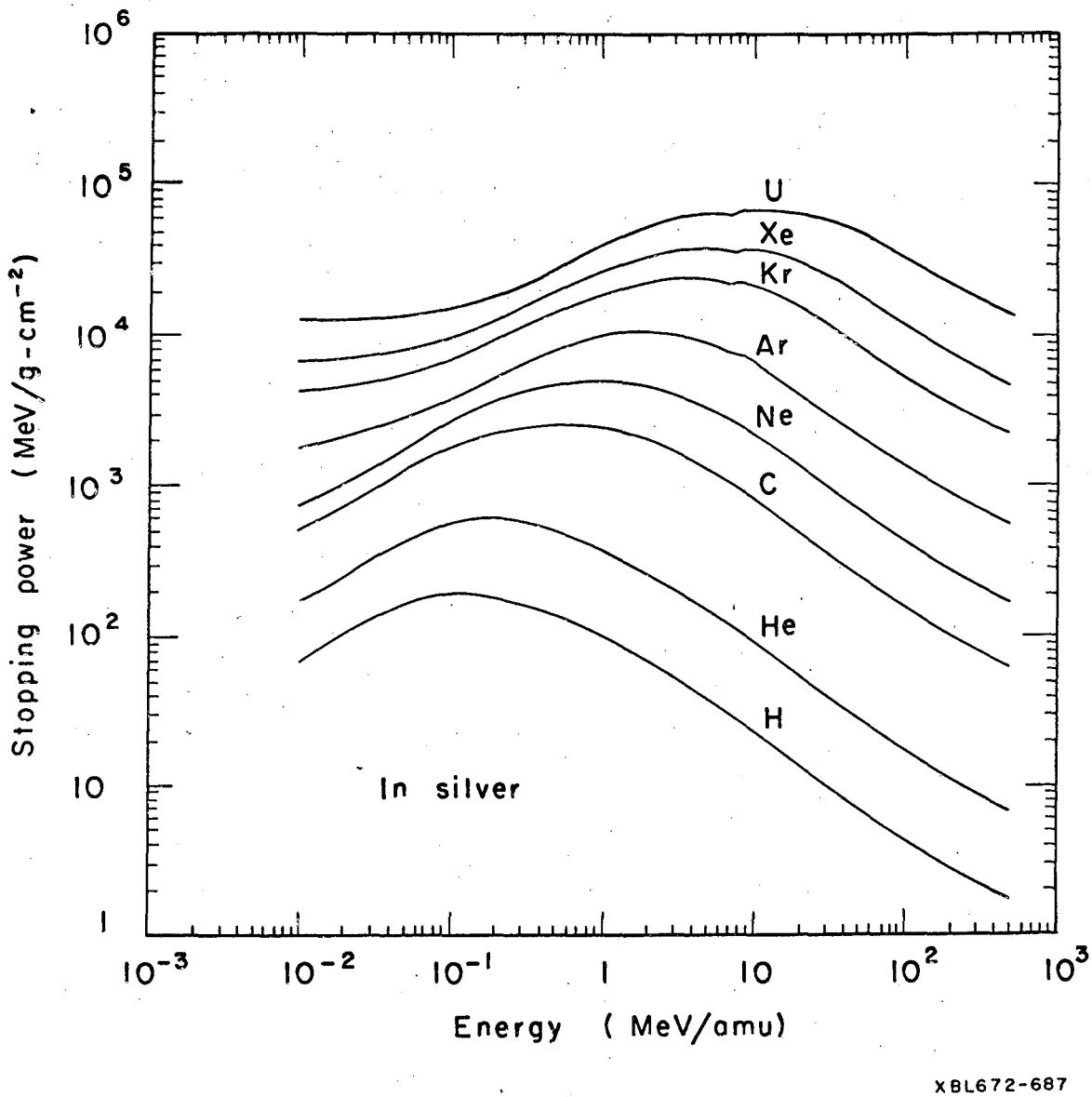

Fig. 10. Stopping-power curves as a function of energy for various ions in silver as calculated by the computer program. The small discontinuity in slope for Kr at 150 MeV/amu is at 137 $\beta = 2Z$, where g becomes 1.0 [see Eq. (19)]. The slight discontinuity at 7 MeV/amu for ions with $Z > 10$ is due to the fact that Eqs. (5) and (6) as employed by Eq. (21) do not match perfectly here.

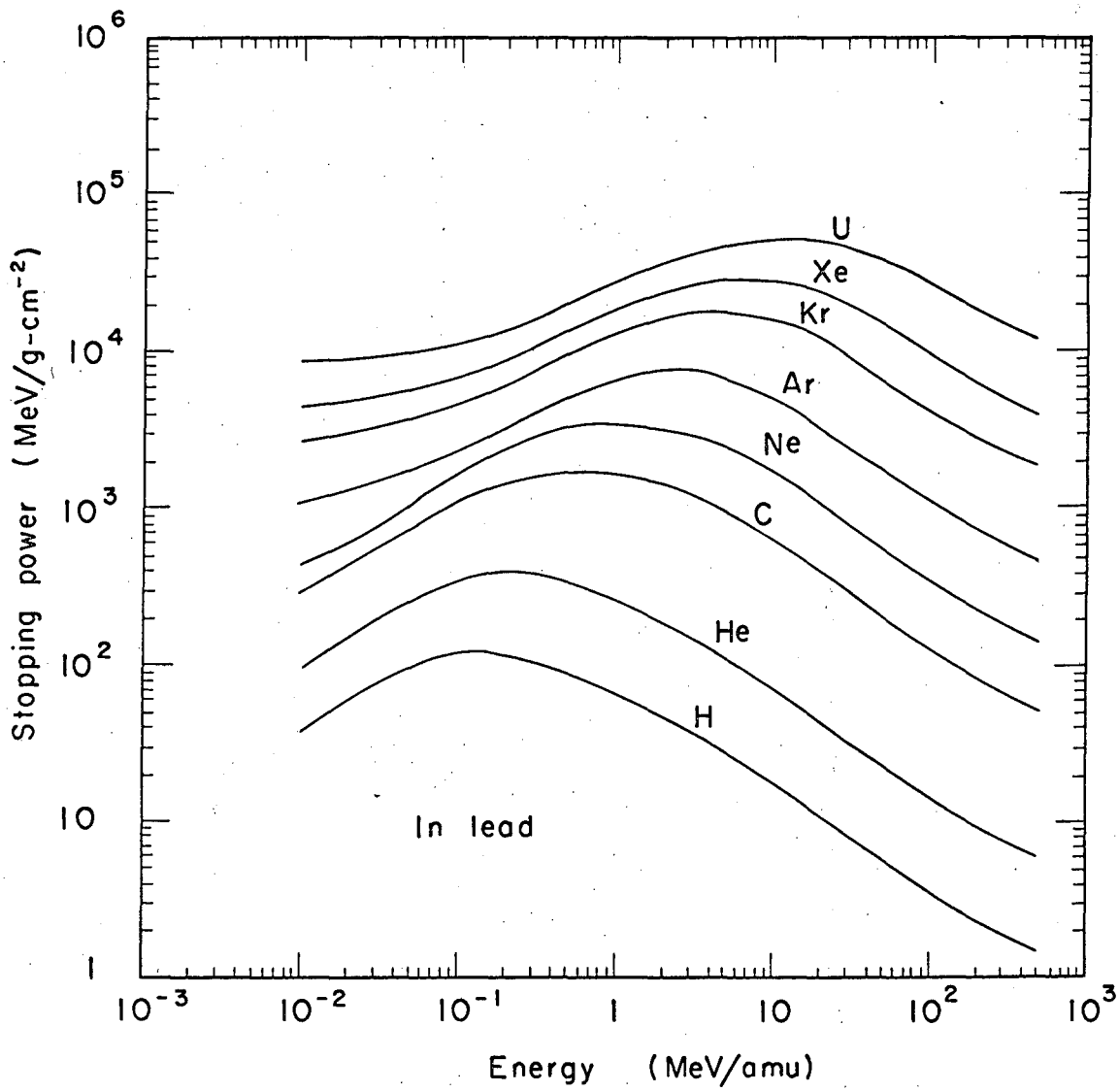

XBL672-688

Fig. 11. Stopping-power curves as a function of energy for various ions in lead as calculated by the computer program. The small discontinuity in slope for Kr at 150 MeV/amu is 137 $\beta = 2Z$, where g becomes 1.0 [see Eq. (19)]. The slight discontinuity at 7 MeV/amu for ions with $Z > 10$ is due to the fact that Eqs. (5) and (6) as employed by Eq. (21) do not match perfectly here.

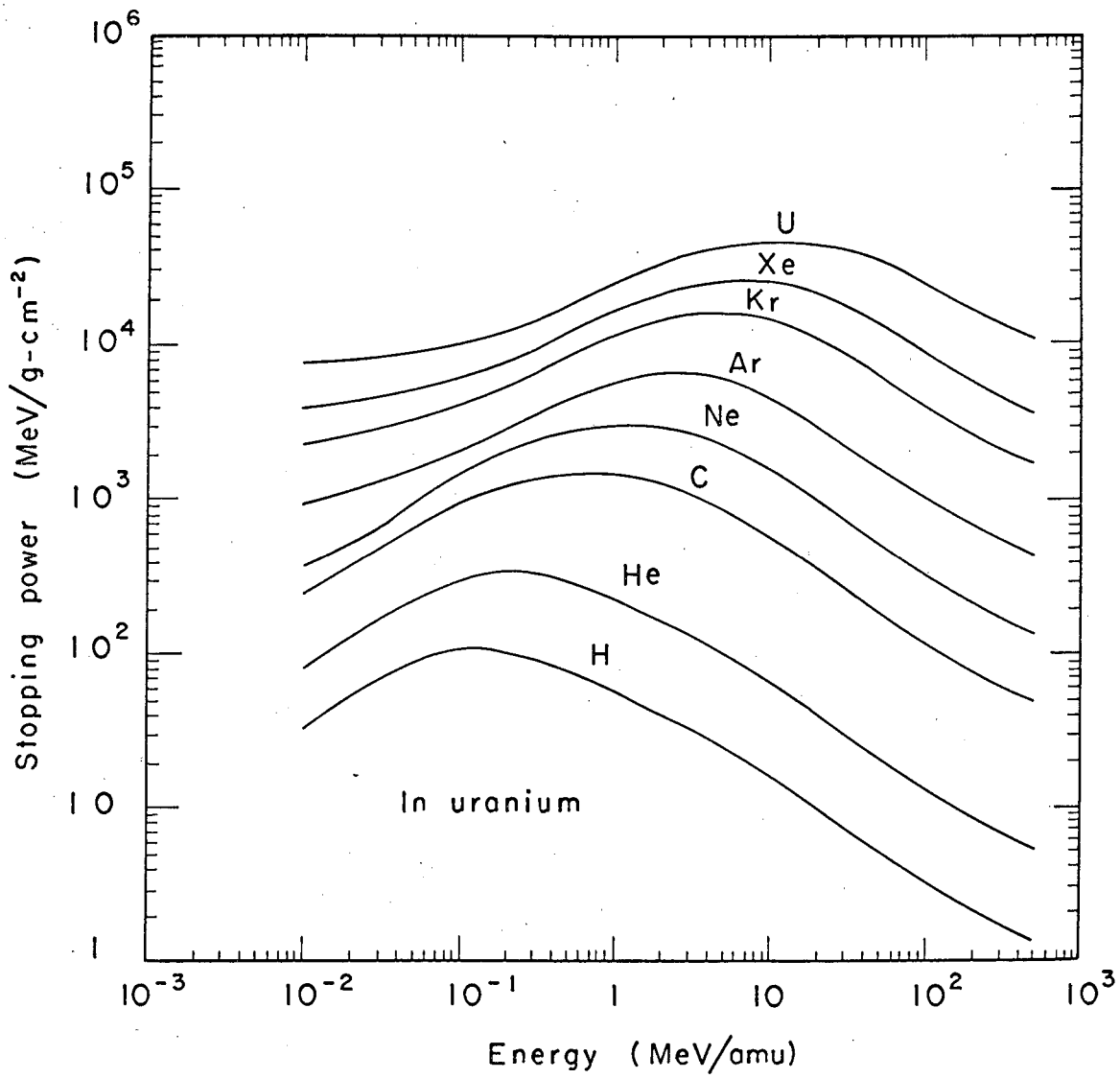

XBL672-689

Fig. 12. Stopping-power curves as a function of energy for various ions in uranium as calculated by the computer program. The small discontinuity in slope for Kr at 150 MeV/amu is 137 $\beta = 2Z$, where g becomes 1.0 [see Eq. (19)]. The slight discontinuity at 7 MeV/amu for ions with $Z > 10$ is due to the fact that Eqs. (5) and (6) as employed by Eq. (21) do not match perfectly here.

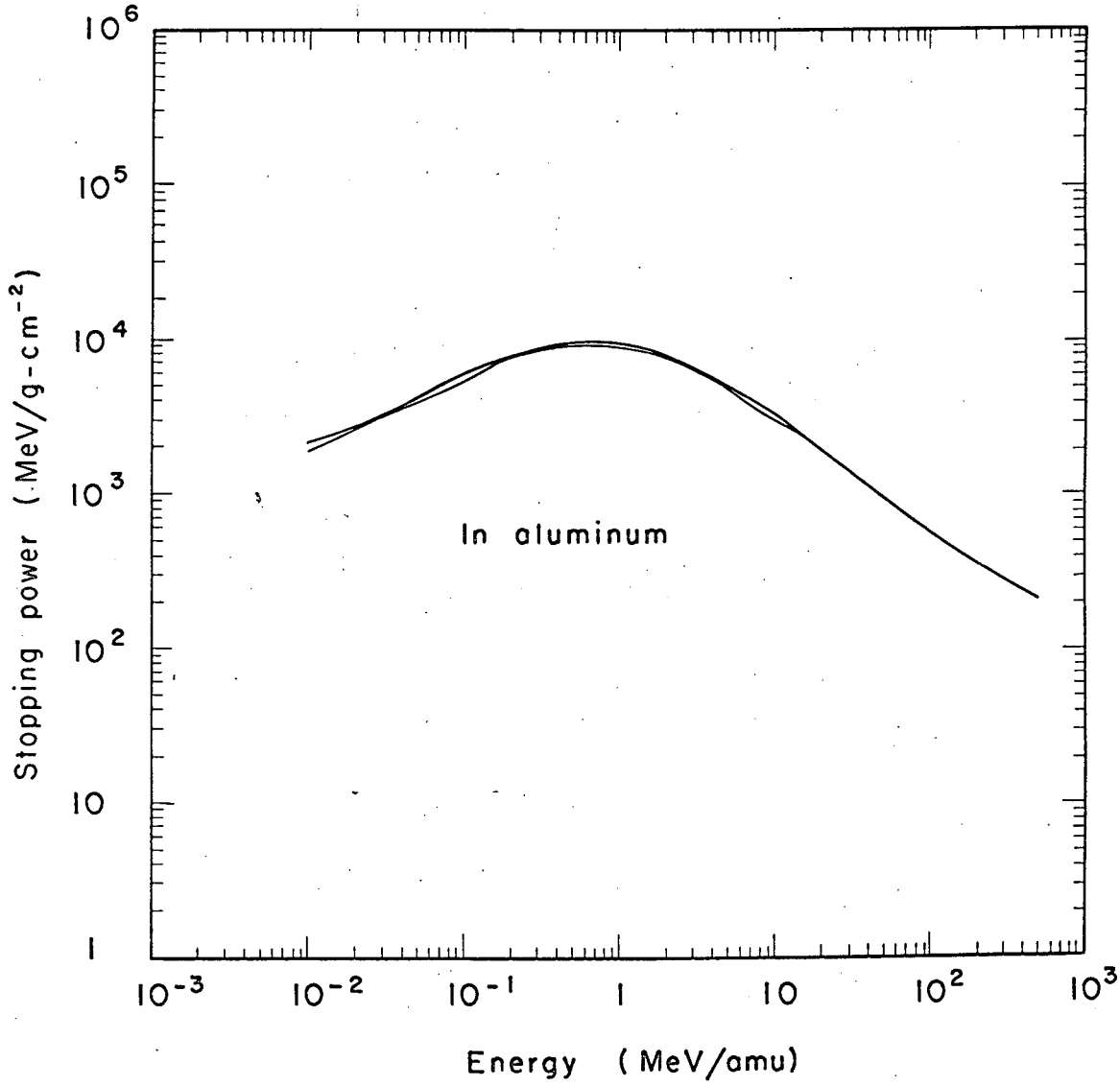

XBL672-675

Fig. 13. Stopping-power curves as a function of energy for neon ions in aluminum. The curve showing a decreasing slope at very low energy is calculated by the method normally used only for ions with $Z > 10$. The other curve is calculated by the method used for $Z \leq 10$. Clearly the discontinuity in the systematic change of stopping-power behavior across the $Z = 10$ boundary (i.e., where we change from one method of calculation to the other) is small.

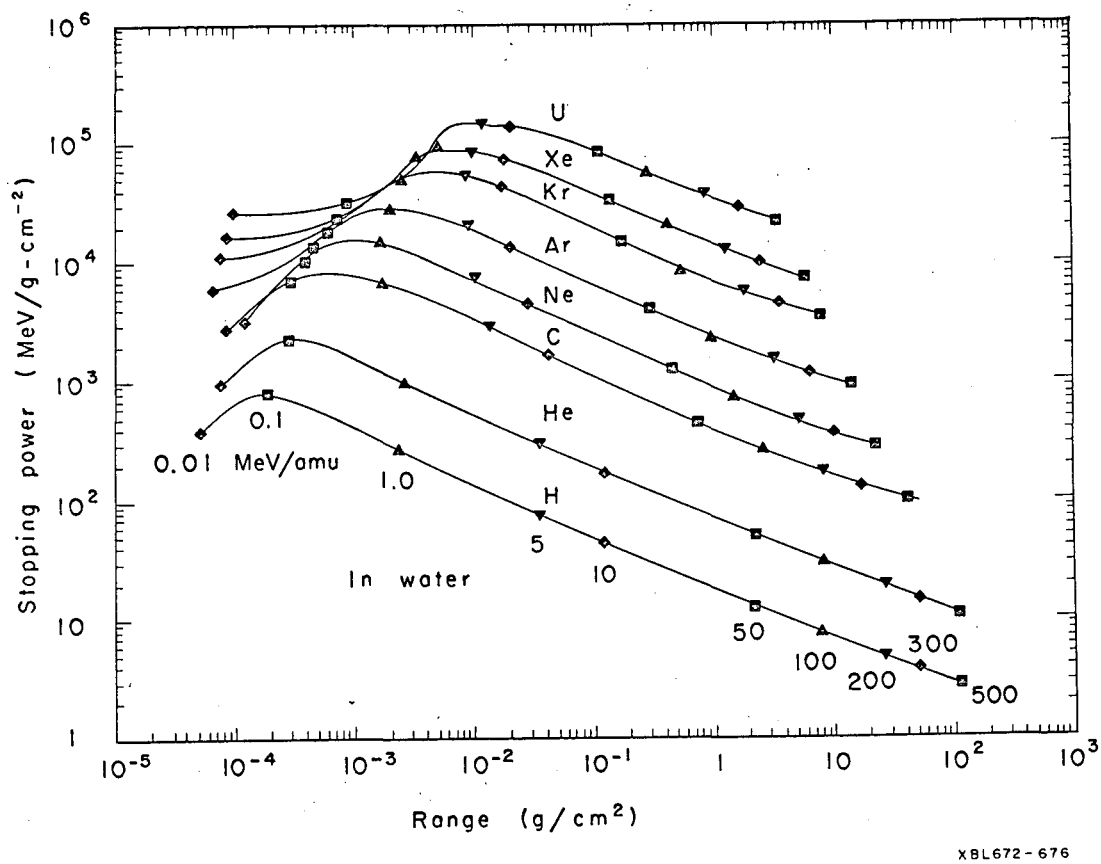

Fig. 14. Stopping-power curves as a function of range for various ions in water as calculated by the computer program. Various ion energies in units of MeV/amu are designated on each curve by the symbols as follows: ◇ left = 0.01, □ left = 0.1, △ left = 1.0, ▽ left = 5.0, ◇ middle = 10, □ middle = 50, △ middle = 100, ▽ middle = 200, ◇ right = 300, □ right = 500. The Ne-C and Xe-U crossovers ar low energy, although possibly a physical reality, occur in regions of low confidence. The stopping power for U at the lower boundary of the medium-high energy region (0.007 g/cm^2) is slightly too large to match well the stopping power at the upper boundary of the low-energy region (0.003 g/cm), as discussed in Sec. IIIB3. The small discontinuity in slope for Kr at 1.2 g/cm^2 is at 137 $\beta = 2Z$, where the function g becomes 1.0 [see Eq. (19)].

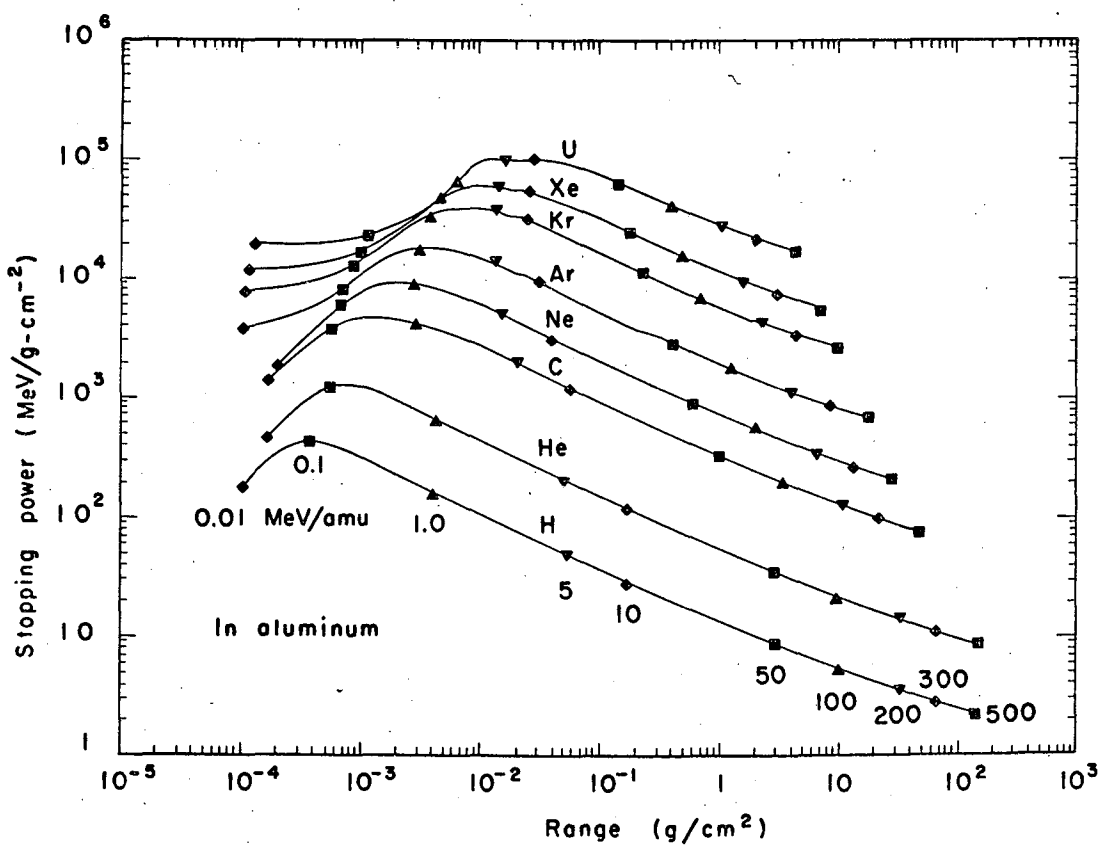

Fig. 15. Stopping-power curves as a function of range for various ions in aluminum as calculated by the computer program. Various ion energies in MeV/amu are designated on each curve by the symbols as follows: ◇ left - 0.01, □ left = 0.1, △ left = 1.0, ▽ left = 5.0, ◇ middle = 10, ⊡ middle = 50, △ middle = 100, ▽ middle = 200, ◇ right = 300, □ right = 500. The slight discontinuity between the 5- and 10-MeV/amu markers for ions with $Z > 10$ is due to the fact that Eqs. (5) and (6) as employed by Eq. (21) do not match perfectly at 7 MeV/amu. The small discontinuity in slope for Kr at 2 g/cm^2 is at 137 $\beta = 2Z$, where the function g becomes 1.0 [see Eq. (19)].

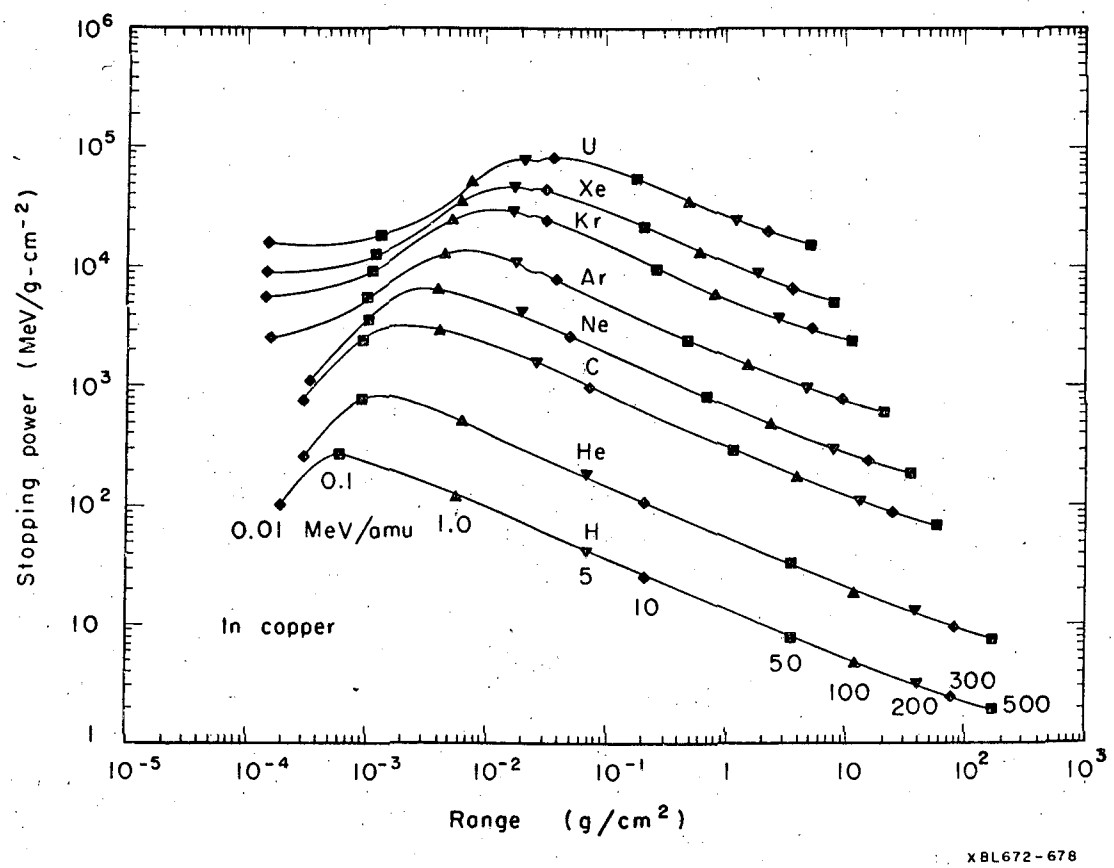

Fig. 16. Stopping-power curves as a function of range for various ions in copper as calculated by the computer program. Various ion energies in units of MeV/amu are designated on each curve by the symbols as follows: ◇ left = 0.01, □ left = 0.1, △ left = 1.0, ▽ left = 5.0, ◇ middle = 10, □ middle = 50, △ middle = 100, ▽ middle = 200, ◇ right = 300, □ right = 500. The slight discontinuity between the 5- and 10-MeV/amu markers for ions with $Z > 10$ is due to the fact that Eqs. (5) and (6) as employed by Eq. (21) do not match perfectly at 7 MeV/amu. The small continuity in slope at Kr at 2 g/cm^2 is at 137 $\beta = 2Z$, where the function g becomes 1.0 [see Eq. (19)].

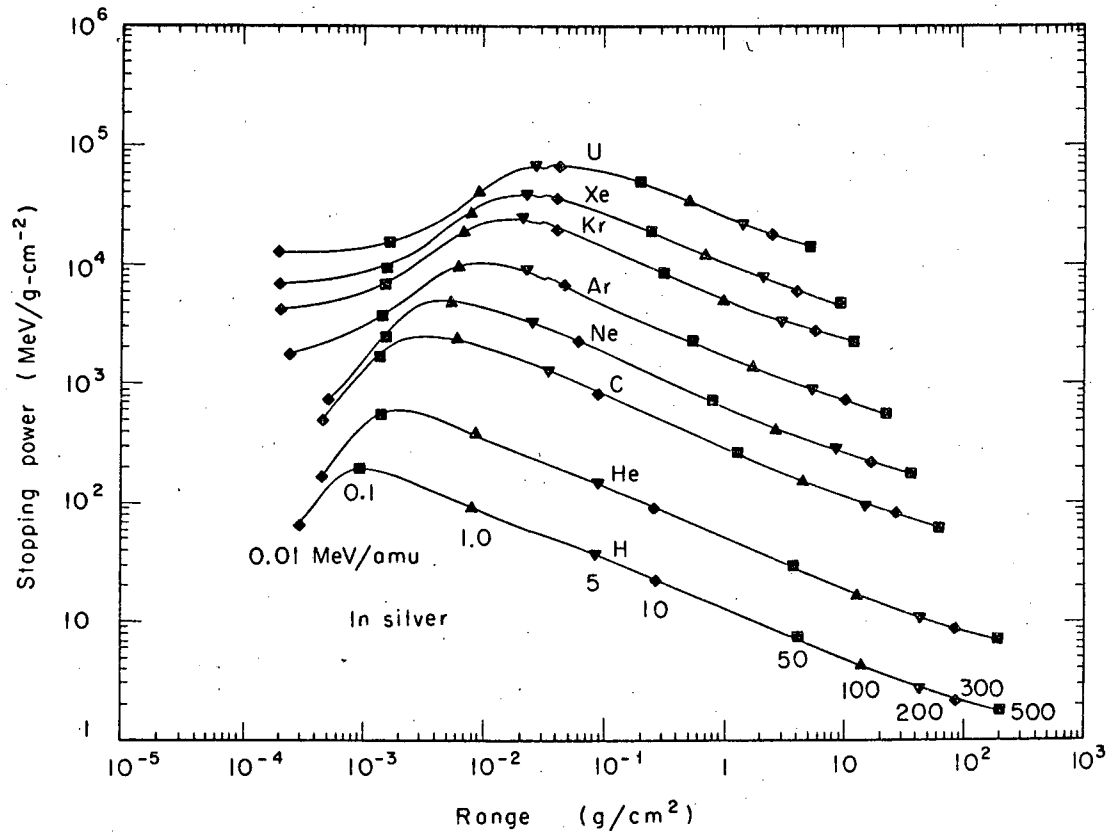

Fig. 17. Stopping-power curves as a function of range for various ions in silver as calculated by the computer program. Various ion energies in units of MeV/amu are designated on each curve by the symbols as follows: ◇ left - 0.01, □ left = 0.1, △ left = 1.0, ▽ left = 5.0, ◇ middle = 10, □ middle = 50, △ middle = 100, ▽ middle = 200, right = 300, □ right = 500. The slight discontinuity between the 5- and 10-MeV/amu markers for ions with $Z > 10$ is due to the fact that Eqs. (5) and (6) as employed by Eq. (21) do not match perfectly at 7 MeV/amu. The small discontinuity in slope for Kr at 2.2 g/cm^2 is at 137 $\beta = 2Z$, where the function g becomes 1.0 [see Eq. (19)].

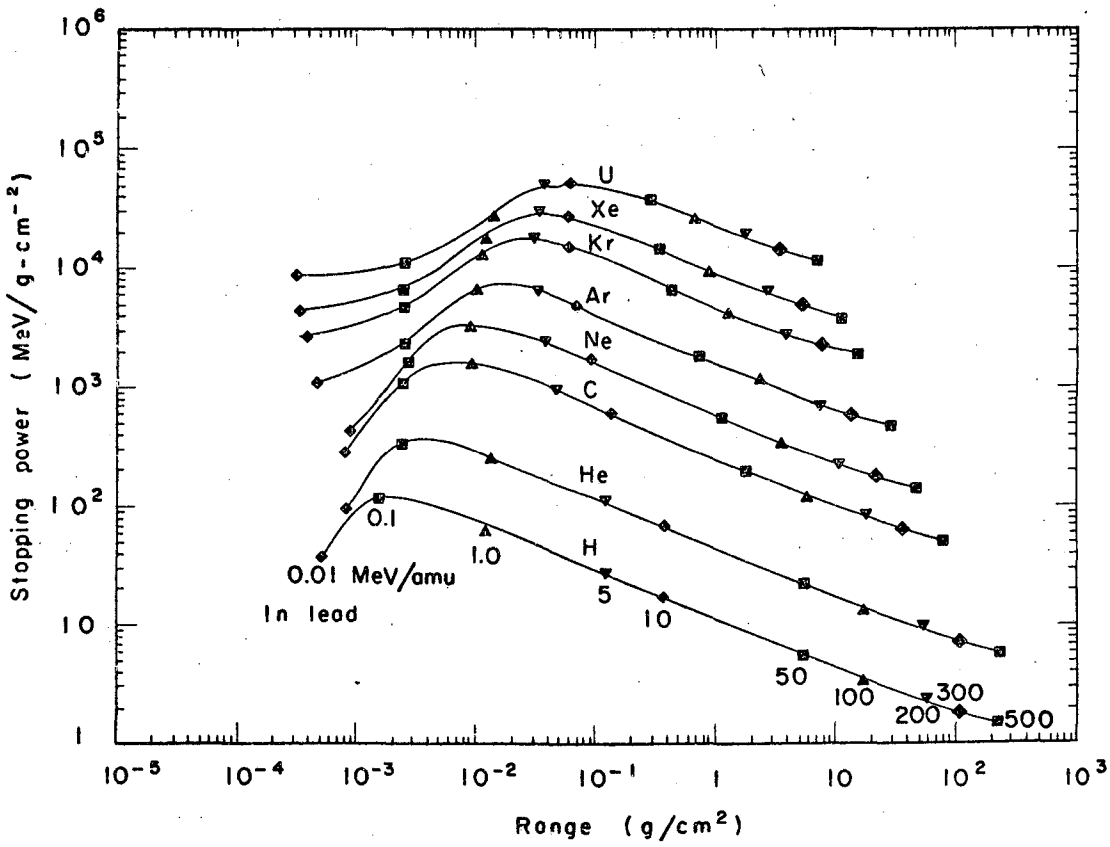

Fig. 18. Stopping-power curves as a function of range for various ions in lead as calculated by the computer program. Various ion energies in units of MeV/amu are designated on each curve by the symbols as follows: ◇ left = 0.01, □ left = 0.1, △ left = 1.0, ▽ left = 5.0, ◇ middle = 10, □ middle = 50, △ middle = 100, ▽ middle = 200, ◇ right = 300, □ right = 500. The slight discontinuity between the 5- and 10-MeV/amu markers for ions with $Z > 10$ is due to the fact that Eqs. (5) and (6) as employed by Eq. (21) do not match perfectly at 7 MeV/amu. The small continuity in slope at Kr at 3 g/cm^2 is at $137\ \beta = 2Z$, where the function g becomes 1.0 [see Eq. (19)].

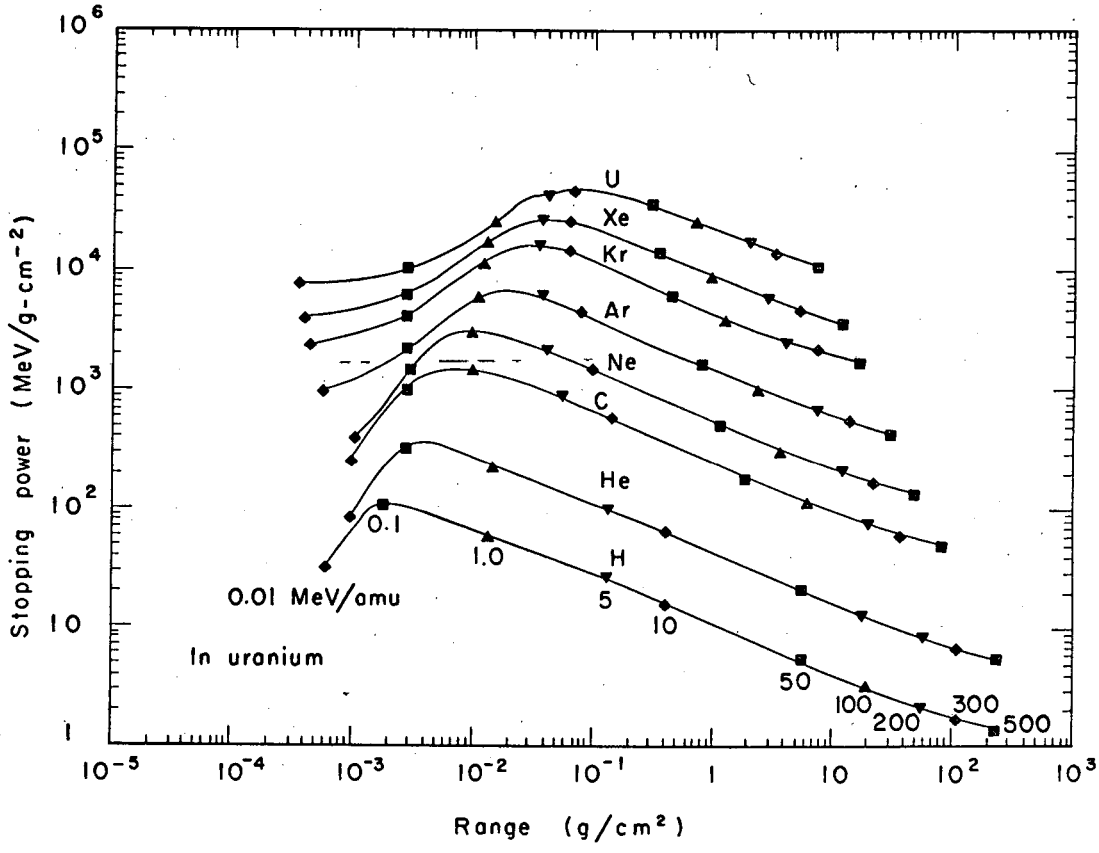

Fig. 19. Stopping-power curves as a function of range for various ions in uranium as calculated by the computer program. Various ion energies in units of MeV/amu are designated on each curve by the symbols as follows: ◇ left = 0.01, □ left = 0.1, △ left = 1.0, ▽ left = 5.0, ◇ middle = 10, □ middle = 50, △ middle = 100, ▽ middle = 200, ◇ right = 300, □ right = 500. The small continuity in slope at Kr at 3.2 g/cm^2 is at 137 β = 2Z, where the function g becomes 1.0 [see Eq. (19)].

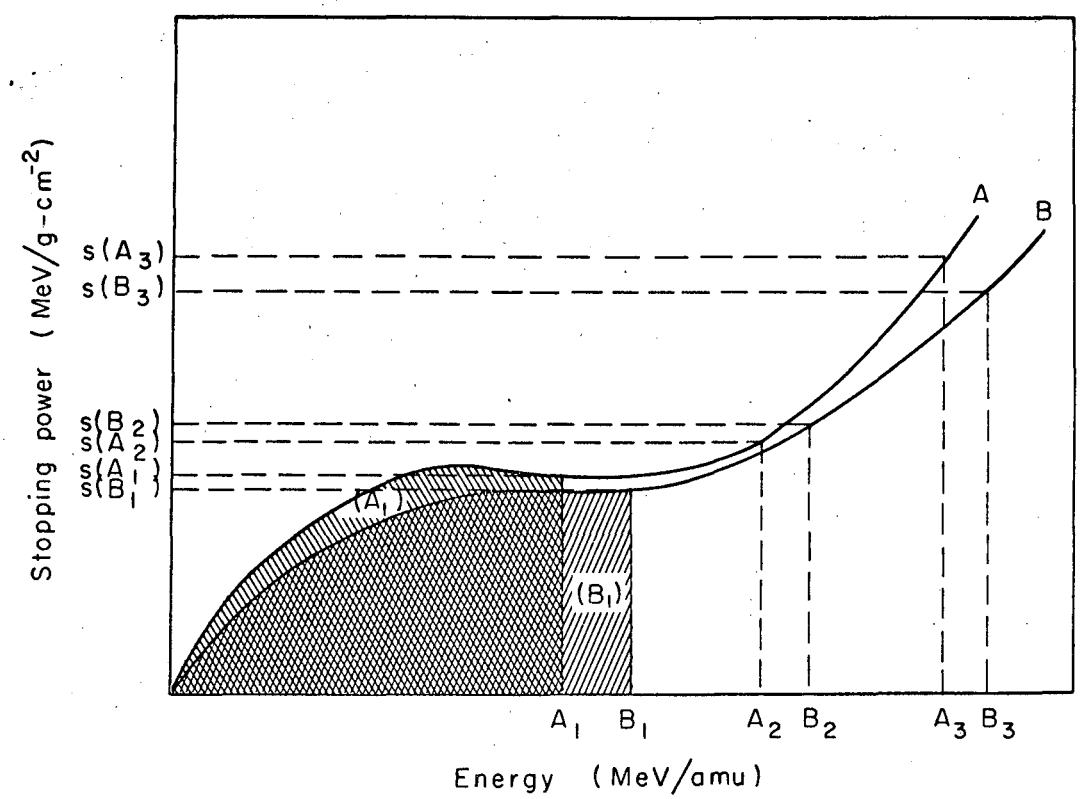

XBL672-690

Fig. 20. Two hypothetical stopping-power curves as a function of energy. These curves show how an increase in the nuclear stopping power for the heavier ion B can cause the stopping power curves for the two ions to cross when plotted as a function of residual range.

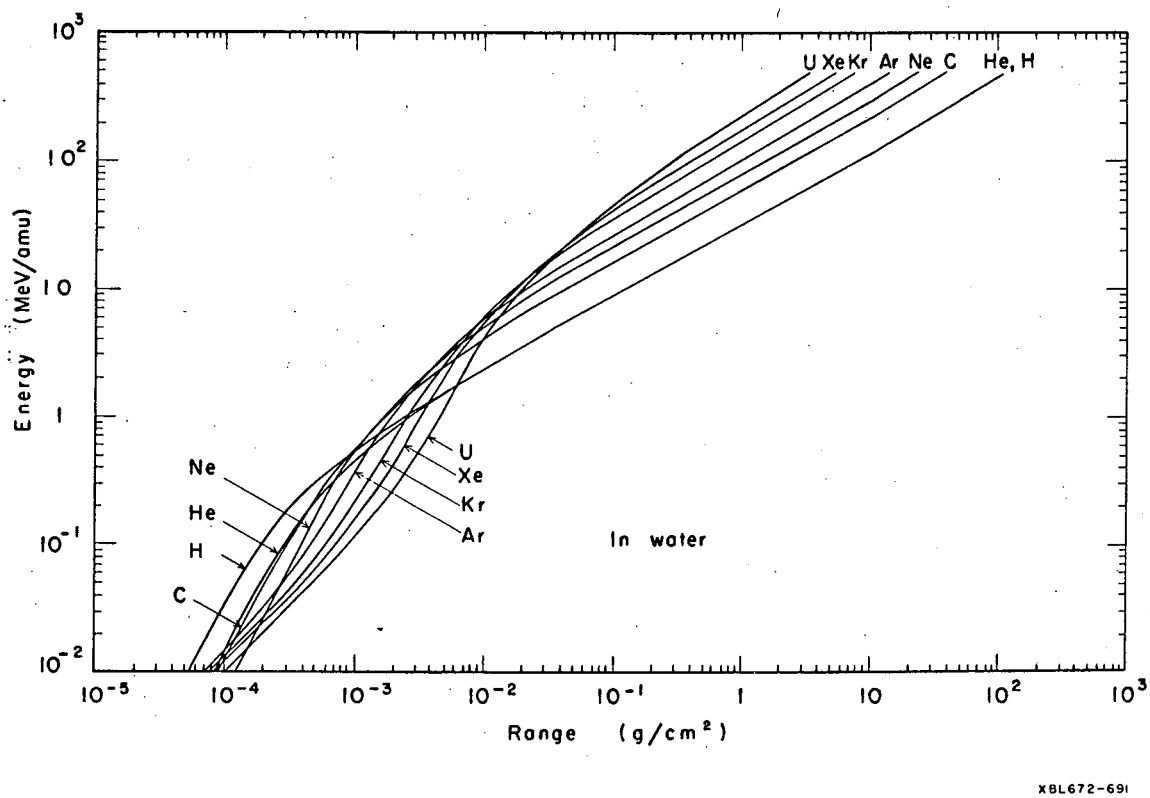

Fig. 21. Energy-range curves for various ions in water as calculated by the computer program. For any energy on the ordinate, the residual range is read from the abscissa. The effect of using completely different methods for calculating the stopping power for the two cases $Z > 10$ and $Z \leq 10$ is apparent for $\epsilon < 0.1$ MeV/amu.

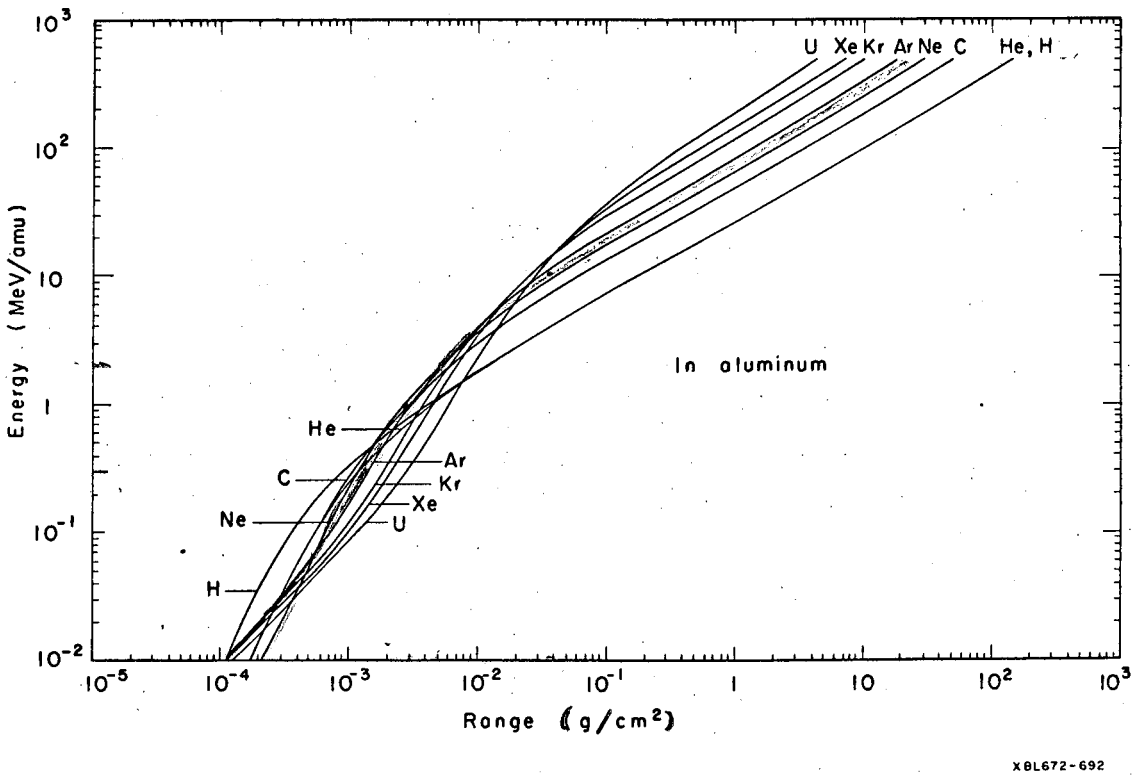

Fig. 22. Energy-range curves for various ions in aluminum as calculated by the computer program. For any energy on the ordinate, the residual range is read from the abscissa. The effect of using completely different methods for calculating the stopping power for the two cases $Z > 10$ and $Z \leq 10$ is apparent for $\epsilon < 0.1$ MeV/amu.

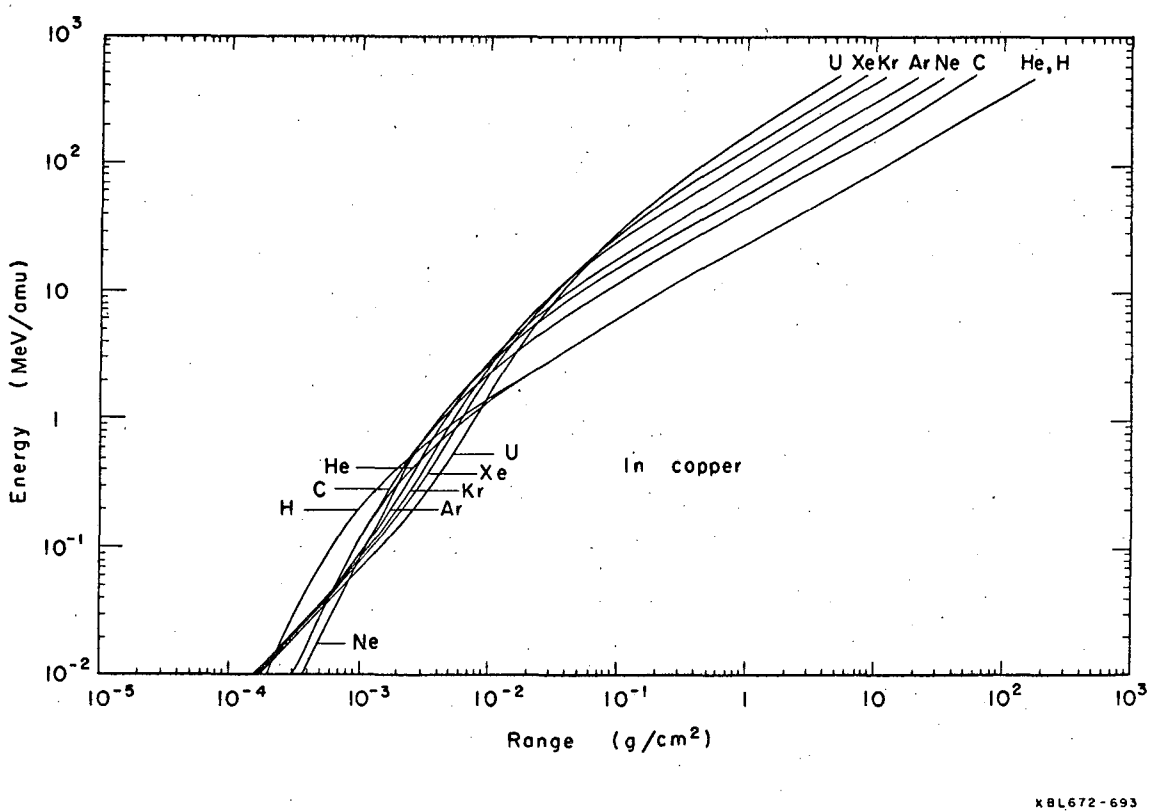

Fig. 23. Energy-range curves for various ions in copper as calculated by the computer program. For any energy on the ordinate, the residual range is read from the abscissa. The effect of using completely different methods for calculating the stopping power for the two cases $Z > 10$ and $Z \lesssim 10$ is apparent for $\epsilon < 0.1$ MeV/amu.

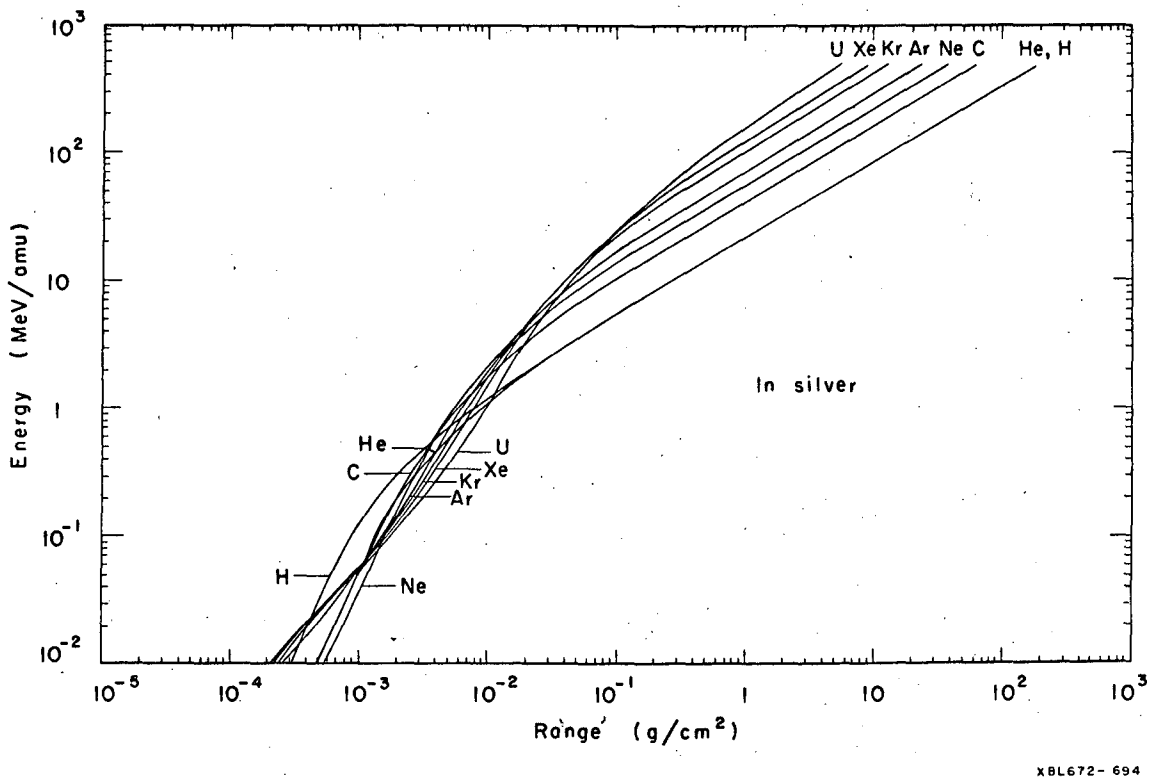

Fig. 24. Energy-range curves for various ions in silver as calculated by the computer program. For any energy on the ordinate, the residual range is read from the abscissa. The effect of using completely different methods for calculating the stopping power for the two cases $Z > 10$ and $Z \leq 10$ is apparent for $\epsilon < 0.1$ MeV/amu.

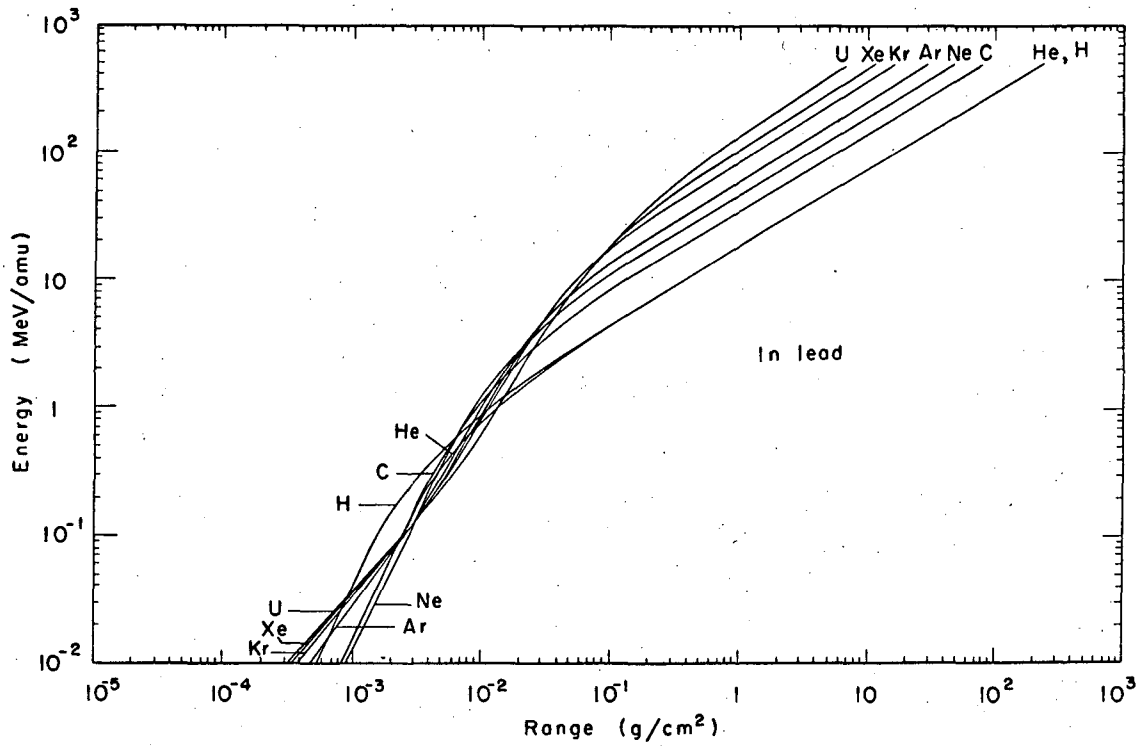

XBL672-695

Fig. 25. Energy-range curves for various ions in lead as calculated by the computer program. For any energy on the ordinate, the residual range is read from the abscissa. The effect of using completely different methods for calculating the stopping power for the two cases $Z > 10$ and $Z \leq 10$ is apparent for $\epsilon < 0.1$ MeV/amu.

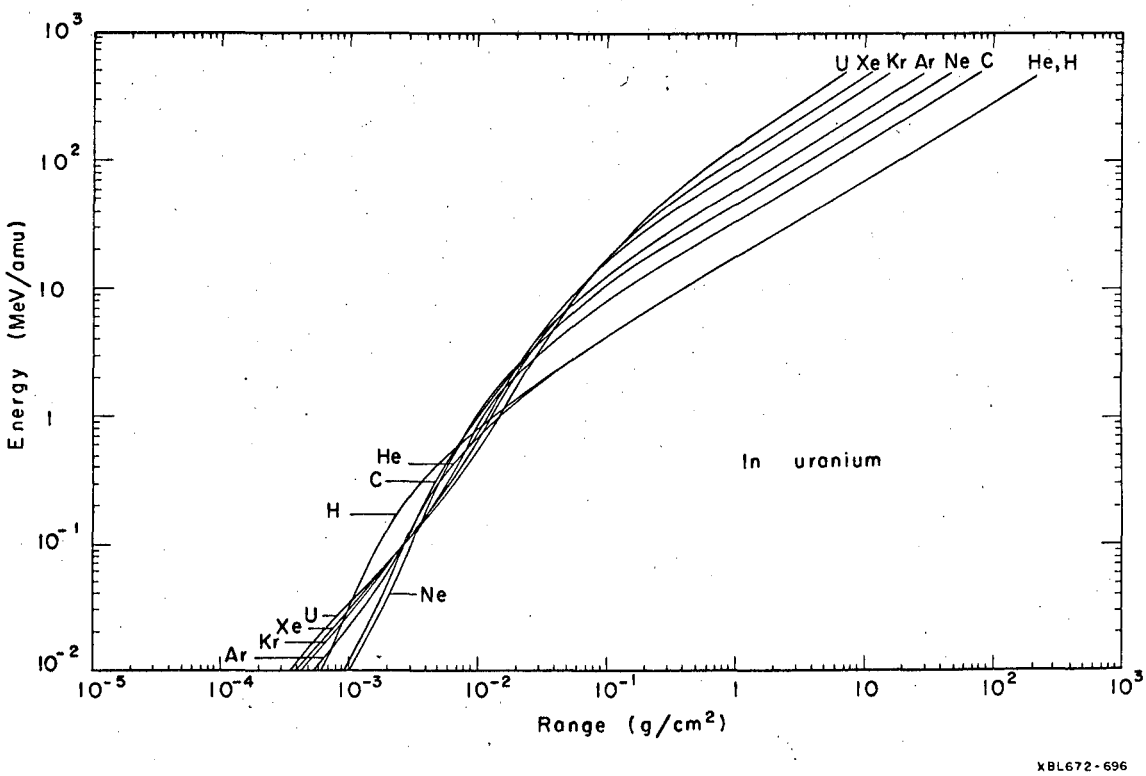

Fig. 26. Energy-range curves for various ions in uranium as calculated by the computer program. For any energy on the ordinate, the residual range is read from the abscissa. The effect of using completely different methods for calculating the stopping power for the two cases $Z > 10$ and $Z \leq 10$ is apparent for $\epsilon < 0.1$ MeV/amu.

This report was prepared as an account of Government sponsored work. Neither the United States, nor the Commission, nor any person acting on behalf of the Commission:

A. Makes any warranty or representation, expressed or implied, with respect to the accuracy, completeness, or usefulness of the information contained in this report, or that the use of any information, apparatus, method, or process disclosed in this report may not infringe privately owned rights; or

B. Assumes any liabilities with respect to the use of, or for damages resulting from the use of any information, apparatus, method, or process disclosed in this report.

As used in the above, "person acting on behalf of the Commission" includes any employee or contractor of the Commission, or employee of such contractor, to the extent that such employee or contractor of the Commission, or employee of such contractor prepares, disseminates, or provides access to, any information pursuant to his employment or contract with the Commission, or his employment with such contractor.